Combining Active Immunization with Monoclonal Antibody Therapy to Facilitate Early Initiation of a Long-acting Anti-methamphetamine Antibody Response

Michael D. Hambuchen[†], **F. Ivy Carroll**[‡], **Daniela Rüedi-Bettschen**[†], **Howard P. Hendrickson**[§], **Leah J. Hennings**[‖], **Bruce E. Blough**[‡], **Lawrence E. Brieaddy**[‡], **Ramakrishna R. Pidaparthi**[‡], and **S. Michael Owens**[*,†]

[†]Department of Pharmacology and Toxicology, College of Medicine, University of Arkansas for Medical Sciences, Little Rock, AR, USA

[‡]Research Triangle Institute, Research Triangle Park, NC, USA

[§]Department of Pharmaceutical Sciences, College of Pharmacy, University of Arkansas for Medical Sciences, Little Rock, AR, USA

[‖]Department of Pathology, University of Arkansas for Medical Sciences, Little Rock, AR, USA

Abstract

We hypothesized that an anti-METH mAb could be used in combination with a METH-conjugate vaccine (MCV) to safely improve the overall quality and magnitude of the anti-METH immune response. The benefits would include immediate onset of action (from the mAb), timely increases in the immune responses (from the combined therapy) and duration of antibody response that could last for months (from the MCV). A novel METH-like hapten (METH-SSOO9) was synthesized and then conjugated to immunocyanin monomers of Keyhole limpet hemocyanin (IC$_{KLH}$) to create the MCV, IC$_{KLH}$-SOO9. The vaccine, in combination with previously discovered anti-METH mAb7F9, was then tested in rats for safety and potential efficacy. The combination antibody therapy allowed safe achievement of an early high anti-METH antibody response, which persisted throughout the study. Indeed, even after four months the METH vaccine

[*]Corresponding Author: Phone: 501-686-5487. Fax: 501-526-4618. mowens@uams.edu.
Present/Current Author Addresses:
Daniela Rüedi-Bettschen, Department of Psychiatry and Human Behavior, University of Mississippi Medical Center, Jackson, Mississippi; Leah J. Hennings, Boehringer Ingelheim Vetmedica, St Joseph, Missouri; Ramakrishna R. Pidaparthi, 9726 Dayton Ct., Raleigh, NC 27617.

antibodies still had the capacity to significantly reduce METH brain concentrations resulting from a 0.56 mg/kg METH dose.

Introduction

Therapeutic anti-(+)-methamphetamine antibodies are under development for the treatment of (+)-methamphetamine (METH) addiction.[1,2] These antibodies are either preformed monoclonal antibodies (mAb) administered intravenously, or polyclonal antibodies (pAb) resulting from active immunization with a METH hapten conjugate vaccine (MCV).[3] Unlike small molecules that modulate the pharmacological effects of METH at neurochemical sites of action within the brain,[4] anti-METH antibodies in the blood stream decrease METH brain effects by reducing and slowing METH's entry across the blood brain barrier.[5]

Although more costly, anti-METH mAbs are advantageous because they can have a half-life of 3–4 weeks in humans and can be dosed in patients to achieve a predictable antibody concentration for potential immediate protection from METH induced effects.[1,2,6] In contrast, a course of carefully timed active immunizations with an MCV over 2–3 or more months can lead to prolonged anti-METH pAb in the vascular circulation.[7,8] Unfortunately during the time period needed for active immunization, patients would not have significant protective levels of anti-METH pAbs, and even the maximum final anti-METH pAb concentrations in the blood stream would be much lower than levels achieved with a mAb.[1,6] In fact, low and variable pAb concentrations following active immunization of humans with nicotine and cocaine conjugate vaccines are considered major reasons for unsuccessful Phase 2 clinical trials.[9,10]

Combining the immediate high levels of protection afforded by anti-METH mAb medication with the long-lasting pAb response from a MCV could provide complimentary therapeutic advantages for patients; including an immediate onset of action (from the mAb), an increased immune response at critical times of relapse to METH (from the combined mAb and MCV), a duration of action lasting for at least several months (from the MCV), and a lower cost of the therapy.

Studies in rats of combined active immunization and mAb therapy for potential treatment of cocaine[11] and nicotine[12,13] abuse show improved overall effectiveness relative to monotherapy in two of three reports. In the cocaine-vaccine study, the anti-cocaine mAb appears to account for the positive results when used in combination with an active vaccination.[11] For each of these studies, the same cocaine- or nicotine-like hapten was used to generate both the exogenously produced mAb and the vaccine used for generating pAb. While not tested in these studies (i.e., mAb was administered 10 or more days after completion of the active vaccination regimen), using the same hapten for producing both antibodies (mAb and pAb) could produce anti-hapten mAb binding to hapten epitopes on the vaccine (free METH hapten) if it is still present. This could lead to a subsequent immune response against the mAb-vaccine complexes.[14,15] This mAb binding to the vaccine could also cause a decreased (or lacking) response to the active immunization.[16,17] Thus, chemical design of unique vaccine hapten structures that are not significantly bound by the administered mAb are needed to prevent potential allergic reactions or mAb neutralization

of the vaccine. Unique hapten antibody specificities for the pAb and mAb could allow safer use of the mAb at earlier time points, including during active immunization.

Producing high affinity, long-acting antibodies against a very small molecular epitope like METH is challenging because unlike large proteins or peptides, METH (149 g/mol) is near the lower limit of molecular size for an immune response. We have previously reported a novel antigen comprised of a carrier protein (*e.g.*, bovine serum albumin [BSA]) conjugated through a linker group at the meta-position of METH's phenyl ring that can generate high affinity, long acting murine antibodies.[18] The best of these anti-METH mAbs is mouse anti-METH mAb7F9 (METH K_d = 7.7 nM).[19] A Phase 1a clinical trial of a chimeric mouse/human form of mouse mAb7F9 has been successfully completed (ClinicalTrials.gov Identifier: NCT01603147).[2] Because of this and murine mAb7F9's established preclinical safety and efficacy profile, it is a lead candidate for combining with a MCV.

To test our hypothesis for combining an anti-METH mAb with a MCV, we generated a new MCV (designated IC_{KLH}-SOO9) with a hapten chemically different from the one used to generate mAb7F9 (Figure 1A).[18] The data from these studies showed that the combined IC_{KLH}-SOO9 and mAb7F9 therapy, over 17 weeks of study, produced early high concentrations of mAb7F9 without hindering active longer-term MCV-induced antibody production or apparent adverse interactions between the MCV and mAb7F9.

Results

Synthesis of MCV and hapten-protein conjugates

Scheme 1 shows the synthesis of the disulfide precursor (**12**, SSOO9) used to generate the desired hapten. (*S,S*)-N-Methylbenzyl-2-methoxyamphetamine (**3**) was synthesized by modification of a method reported for other similar compounds.[20] Thus, reductive alkylation of *o*-methoxyphenylacetone (**1**) with (*S*)-(-)-α-methylbenzylamine using triacetoxyborohydride in ethylene dichloride gave a mixture of (*R,S*)- and (*S,S*)-**3** in a 1:2 ratio. Recrystallation of the hydrochloride salts of the mixture from toluene gave pure (*S,S*)-**3** which was converted to the *N*-formyl intermediate **4** using a formic acid/acetic anhydride mixture. Reduction of **4** using diborane in tetrahydrofuran provided the *N*-methyl compound **5**. Subjection of **5** to transfer hydrogenation using ammonium formate and 5% palladium on carbon catalyst in methanol yielded **6**. *O*-Demethylation of **6** using boron tribromide in methylene chloride afforded the phenol **7**. Treatment of **7** with di-*tert*-butyl dicarbonate in methanol containing triethylamine at 50 °C for 2.5 h gave **8**. The sodium salt of **8** prepared using sodium hydride in dimethylformamide was used to alkylate methyl 6-bromohexanoate to give **9**. Hydrolysis of **9** using aqueous lithium hydroxide afforded **10**. Coupling of **10** with cystamine dihydrochloride using hexa-(benzotriazol-1-yloxy)tris (dimethylamino)phosphanium hepafluorophosphate (BOP) in tetrahydrofuran containing triethylamine gave the protected disulfide **11**. Treatment of **11** with 2N hydrochloride acid yielded the desired **12** (SSOO9).

Scheme 2 outlines the synthesis of the disulfide precursor (**15**, SSMO9) that was used to prepare the SMO9 that was used to synthesize IC_{KLH}-SMO9. Thus, coupling of **13**[21] with cystamine dihydrochloride using BOP in tetrahydrofuran containing triethylamine afforded

14. Treatment of **14** with an etheral solution of hydrogen chloride yielded the desired **15** (SSMO9).

The synthesis of IC_{KLH}-SOO9 and IC_{KLH}-SMO9 are shown in Scheme 3. Treatment of IC_{KLH} (**16**) with sulfo-SMCC (**17**) in water gave the maleimide-activated IC_{KLH} (**18**). To prepare the METH hapten protein conjugate, the SSOO9 (**12**) and SSMO9 (**15**) were first reduced with tris(2-carboxyethyl)phosphine (TCEP) and the resulting mercaptans then added to the maleimide-activated IC_{KLH} (**18**) to give IC_{KLH}-SOO9-MCV (**19**) and IC_{KLH}-SMO9 MCV (**20**). The IC_{KLH}-SOO9-MCV used for *in vivo* studies was determined to have 26 SOO9 haptens incorporated per IC_{KLH}.[22] Conjugation of the haptens derived from SSOO9 and SSMO9 to the Imject Maleimide Activated ovalbumin (OVA) carrier protein for enzyme-linked immunosorbent assay (ELISA) was performed similarly minus the carrier protein activation steps. OVA-SOO9 was determined to have 11 haptens incorporated, and OVA-SMO9 was determined to have 9 haptens incorporated.

Selection of optimal combination of anti-METH mAb and IC_{KLH}-METH hapten conjugate by *in vitro* immunochemical analysis

In previous reports, both anti-METH mAb7F9 and mAb4G9 were shown to have an excellent safety and efficacy profile during preclinical testing,[19,23] however the preponderance of the *in vitro* and *in vivo* data indicated mAb7F9 was the better of the two mAbs for taking forward to clinical trials. For human clinical trials it was converted to a chimeric (mouse-human) anti-METH mAb.[2,19]

In preparation for the current studies, we retested both mAb7F9 (generated from BSA-MO9, Figure 1Aiii.) and mAb4G9 (generated from OVA-MO9, Figure 1Aiv.) for their cross-reactivity against two new MCVs, IC_{KLH}-SMO9 and IC_{KLH}-SOO9 (Figure 1Ai. and 1Aii.). These immunological cross-reactivity data helped to make our final choice of the best mAb + MCV combination for our studies.

Both IC_{KLH}-SMO9 and IC_{KLH}-SOO9 (Figure 1Ai and 1Aii) showed similar half maximal inhibitory concentration (IC_{50}) values for inhibition of [3H]-METH binding to anti-METH mAb4G9 (Figure 1B), which predicted there would be a significant amount of cross reactivity *in vivo*. In contrast, the IC_{50} values for IC_{KLH}-SMO9 inhibition of [3H]-METH binding to mAb7F9 were approximately 10 times lower than those for IC_{KLH}-SOO9. These *in vitro* data suggested that the combination of IC_{KLH}-SOO9 as a MCV with mAb7F9 would yield the least *in vivo* cross reactivity and thus maximal antibody concentrations and safety. Note that in previous publications we referred to the MO9 hapten as MO10. We have since changed this hapten nomenclature to be MO9 to reduce confusion of the total number of linear spacer molecules between the METH backbone structure and the antigenic carrier protein.

Combined anti-METH pAb and mAb7F9 [3H]-METH binding

Figure 2 compares results from rapid equilibrium dialysis (RED) measurements of [3H]-METH binding titers (at a 1:50 dilution) of serum samples from rats in each group. The dosing schedule is described in Figure 2, and note that the IC_{KLH}-SOO9 + mAb7F9

combination treated group was administered all treatments (mAb and MCV) listed. At weeks 5, 15, and 17, serum METH binding data in IC_{KLH}-SOO9 + mAb7F9 combination and IC_{KLH}-SOO9-only treated animals were not significantly different, but both had significantly elevated [^{3}H]-METH binding compared to the animals in the mAb7F9 group (p<0.05). At weeks 8 and 9, [^{3}H]-METH binding measurements in IC_{KLH}-SOO9 + mAb7F9 combination treated and mAb7F9-only treated animals were not significantly different, but both had significantly elevated [^{3}H]-METH binding compared to the animals in the IC_{KLH}-SOO9-only treated group (p<0.05). At week 11, two weeks after the second MCV booster immunization, [^{3}H]-METH binding in the IC_{KLH}-SOO9 + mAb7F9 combination group alone was significantly elevated compared to the IC_{KLH}-SOO9-only treated rats (p<0.05). By week 17, serum [^{3}H]-METH binding in the mAb7F9-only treated group was not significantly different from pretreatment, baseline values.

Presence of anti-METH pAbs and (or) mAb7F9

Figure 3 shows the ELISA measurements of serum from the mAb7F9-treated group (week 8) with the anti-mouse secondary antibody on OVA-SOO9 coated plates. No substantive hapten-specific mAb7F9 binding occurred. Figure 4 shows the ELISA measurements of IC_{KLH}-SOO9-induced rat pAb (left panel) or mouse mAb7F9 (right panel). The values for the area under the 405 nm absorbance vs. serum dilution curve for all dilutions (AUC) was used to make statistical comparisons. At all time points, weeks 8, 11, and 17, the measurement of rat antibodies generated from IC_{KLH}-SOO9 immunizations (left panel of Figure 4) showed that the IC_{KLH}-SOO9 + mAb7F9 combination and IC_{KLH}-SOO9-only treated rat AUC values were not significantly different. In contrast, the AUC values resulting from both treatments were significantly elevated compared to the values of the mAb7F9-only treated animals (p<0.05). On weeks 8 and 11, the mAb7F9 AUC data (right panel of Figure 4) showed IC_{KLH}-SOO9 + mAb7F9 combination and mAb7F9-only treated animal AUC values were not significantly different, but were both significantly elevated compared to the AUC values of the IC_{KLH}-SOO9-only treated animals (p<0.05). There were no differences in mAb7F9 binding between any of the groups on week 17.

Note that the data sets in each panel of Figure 4 were not intended for comparisons between time points or antibody types (mAb7F9 vs. pAb). It was intended to show the overall anti-METH antibody response in the serum from each of the three treatment groups (*e.g.,* was a mAb7F9 response present or not).

Average affinity values of the anti-METH pAb for METH

In week 17 rat serum, the average affinity of pAb in IC_{KLH}-SOO9-only and IC_{KLH}-SOO9 + mAb7F9 treated rats was not significantly different (K_d = 21.8 ± 8.4 and 30.1 ± 10.7 nM, respectively).

METH serum and brain concentrations after a 0.56 mg/kg METH challenge dose

At study week 11, 2 hrs after a 0.56 mg/kg METH challenge, METH serum concentrations in the IC_{KLH}-SOO9-only, mAb7F9-only, and IC_{KLH}-SOO9 + mAb7F9 combination treated animals were not significantly different (Figure 5). On week 17, 2 hrs after an additional 0.56 mg/kg METH challenge, the serum and brain concentration values in the mAb7F9-only

treated animals were not significantly different from identically challenged historical control values from our laboratory (from rats immunized with activated-IC_{KLH}, data not shown). Serum METH concentrations in the IC_{KLH}-SOO9-only and IC_{KLH}-SOO9 + mAb7F9 combination treatment groups were not significantly different from each other, but were both significantly elevated compared to the concentrations in the mAb7F9 treatment group ($p<0.05$). Importantly, on week 17 (at the end of the studies) whole brain METH concentrations in the IC_{KLH}-SOO9-only and IC_{KLH}-SOO9 + mAb7F9 combination treatment groups were not significantly different from each other, but were both significantly reduced compared to the concentrations in the mAb7F9 treatment group ($p<0.05$). This showed the capacity of the MCV to produce long-term reductions in METH concentrations in the brain. Amphetamine (AMP, a pharmacologically active METH metabolite) serum and brain concentrations were not significantly different between the three groups at any of the post-METH challenge collection times. IC_{KLH}-SOO9-only, mAb7F9-only, and IC_{KLH}-SOO9 + mAb7F9 treated rats, respectively, had serum AMP concentrations of 10 ± 2, 10 ± 2, and 11 ± 3 ng/ml at week 11 and 11 ± 4, 8 ± 2, and 11 ± 3 ng/ml at week 17. Brain AMP concentrations at week 17 were 80 ± 19, 98 ± 20, and 82 ± 16 ng/g in these three groups, respectively.

Safety assessment

Animal weights and rectal temperatures relative to baseline were not different between any of the groups at any time point during the study (Figure 6A and 6B). At the termination of the experiment, no gross lesions were observed at the immunization site, heart, thymus, lymph nodes, liver, intestines, adrenals, or spleen in any animals. Approximately half the animals from each group exhibited mild mottling of the lung but there was no difference in frequency of this lesion between groups. Lung mottling was likely an artifact of the anesthesia used during animal procedures. One animal in the IC_{KLH}-SOO9-only group had kidney mottling, but there was no incidence of this in the other groups. In addition, organ weights of the heart, liver, kidney, and spleen were not different between the groups (Figure 6C).

Discussion

By carefully pre-selecting an anti-METH mAb for maximal compatibility with minimal cross-reactivity against the IC_{KLH}-SOO9 MCV, we increased our chances for success (Figure 1). The choice of mAb7F9 and IC_{KLH}-SOO9 MCV was confirmed based on results of the testing of the rat serum samples collected over time from each test group (Figures 2–5). The combination treatment showed no indication that it was unsafe, because there was no substantive difference between the treatment groups (Figure 6) in terms of changes in body weight, temperature, or organ weight (determined at week 17). The gross pathology of the organs showed no differences or apparent abnormalities in the groups. We also had additional confidence in the use of murine mAb7F9 in these studies since the chimeric mouse/human form of mAb7F9 has successfully completed an FDA Phase 1a clinical trial.[2]

The MCV (IC_{KLH}-SOO9) was designed to generate pAbs that would be selective for the (+)-isomer of METH, since the (−)-METH stereoisomer is not a pharmacologically active

stimulant drug of abuse.[24] To accomplish this goal we confined the chemical sites for the addition of a linker group to METH's phenyl ring structure, because attachment of a linker group near the chiral center of METH would likely result in antibodies that were not selective between (+)-METH and (−)-METH. We did not consider the para position on the phenyl ring structure of (+)-METH as a site for the hapten linker attachment because conjugation at this site can produce anti-METH mAbs that are inactivated *in vivo*.[25] A meta-linked hapten was used to generate mAb7F9 (and mAb4G9), so this site of attachment was ruled out because we were concerned that a meta linked MCV would significantly bind anti-METH mAb7F9 *in vivo* (see Figure 1B). We reasoned our best choice for a suitable MCV was to attach the linker side chain to the ortho-position of (+)-METH's phenyl ring structure.

For the rat studies we had three treatment groups consisting of IC_{KLH}-SOO9-only, mAb7F9-only and IC_{KLH}-SOO9 + mAb7F9 combined therapy. Rats receiving the MCV were first immunized and then boosted (at 3 weeks) with the MCV. This allowed establishment of an initial immunological response. Based on this response (measurements at week 5), the MCV vaccinated rats were match-paired into balanced MCV-only and MCV + mAb7F9 groups prior to the administration of mAb7F9 at weeks 6 and 7 (to both the mAb7F9-only and MCV + mAb7F9 groups). Two more booster immunizations were administered to the MCV treated groups at weeks 9 and 15 (Figure 2). This experimental strategy was designed to test for undesirable potential *in vivo* cross-reactivity between mAb7F9 and IC_{KLH}-SOO9 proteins resulting in adverse reactions or neutralization of the active anti-METH pAb response.

The rats in the mAb7F9-only and IC_{KLH}-SOO9 + mAb7F9 treated groups had substantial increases in [³H]-METH binding after mAb7F9 dosing (Figure 2), which showed the potential for mAb7F9 to quickly initiate high levels of anti-METH binding. This would be clinically important since we envision that a rapid initiation of anti-METH antibody response would be beneficial for treating METH addiction and relapse to METH use. Despite these high early mAb7F9 concentrations, there were no apparent mAb7F9 and MCV interactions resulting in decreased anti-METH pAb production (Figure 4, Weeks 8 and 11).

Indeed, starting after the first mAb7F9 dose on week 6 and lasting until week 11, the mAb7F9 + MCV combination produced significantly greater anti-METH antibody binding of [³H]-METH than the MCV alone (Figure 2). In the mAb7F9-only compared to MCV-only treated rats, however, the statistically significant elevation in [³H]-METH binding was lost prior to week 11. Therefore, the use of anti-METH mAb supplemental dosing could substantially enhance a weak response after MCV immunizations or in immune comprised patients (*e.g.*, due to AIDS). There was no difference in [³H]-METH binding between the mAb7F9 + MCV combination- and mAb7F9-treated groups in the time points measured from week 8–11 (Figure 2), despite the presence of pAb in the serum of the mAb7F9 + MCV combination-treated group (Figure 4 left panels). This was likely due to the endogenously produced pAb binding being overshadowed by the higher concentration, higher affinity mAb7F9 binding (7.7 nM vs 21.8–30.1 nM for the pAb) prior to substantial elimination of mAb7F9.[19]

The IC_{KLH}-SOO9-only and IC_{KLH}-SOO9 + mAb7F9 combination treatments had longer-lasting elevation of [^{3}H]-METH binding titers (determined on weeks 15 and 17), which was well beyond the time course for similar binding in the mAb7F9-only group, and there was no significant difference in binding titers between the MCV-only and combination treatment groups (Figure 2). The ELISA results showed that the prolonged [^{3}H]-METH binding in the combination treated rats (Figure 2) was due to the pAb response generated by active immunization with IC_{KLH}-SOO9 MCV rather than residual mAb7F9 concentrations (Figure 4, left and right panels, Week 17) and that there was no significant differences in anti-METH pAb binding titers between the combination and MCV-only groups (Figure 4, left panel, Week 17). Additionally, at week 17, there was no significant difference in average METH affinity of pAbs generated by active vaccination in the IC_{KLH}-SOO9-only and IC_{KLH}-SOO9 + mAb7F9 combination treated rats (K_d = 21.8 and 30.1 nM, respectively). While the affinity of these pAbs for METH was lower than previously shown in a study of another anti-METH vaccine from our group, IC_{KLH}-SMO9 (K_d = 13.7 nM),[3] they were comparable to those generated by other investigators of active anti-METH vaccination therapy (K_d = 30.4).[26] Overall, these binding data in Figures 2 and 4 confirmed that treatment with mAb7F9 at weeks 6 and 7 resulted in early anti-METH antibody effects and did not hinder the continued immune response resulting from booster MCV immunizations at week 3, the peak response to the MCV after the boost at week 9, and the continuation of the peak response after the boost at week 15 (shown as both pAb concentration and affinity).

On week 17 when the mAb7F9 [^{3}H]-METH binding was insignificant (*i.e.*, not different from pre-immunization values, Figure 2) and mAb7F9 titers in the both groups treated with the mAb were not different than those in the MCV-only treated group (Figure 4, right panel, week 17), we administered a dose of METH (0.56 mg/kg) to determine if the anti-METH pAb binding capacity was sufficient to reduce METH concentrations in the brains of the rats. Compared to the mAb7F9-only treated group, both the IC_{KLH}-SOO9-only and IC_{KLH}-SOO9 + mAb7F9 combination treatments significantly increased METH concentrations in the serum and significantly decreased whole brain METH concentrations 2 hrs after the 0.56 mg/kg METH dose (Figure 5) on week 17. Note that the serum and brain concentrations in mAb7F9 treated rats were not different from historical control values in our laboratory. These antibody-induced reductions in METH brain concentrations demonstrated both the MCV's inhibitory effect on METH penetration of the CNS and further evidence of the lack of interaction between the MCV and mAb7F9. Similar reductions in brain METH concentrations were found in a previous study using anti-METH mAb7F9 and a challenge dose of 1.68 mg/kg METH two weeks after mAb administration (37% vs ~31% in the current study). In this previous study the reductions in METH brain concentrations correlated with a 31% decrease in the duration of METH-induced distance traveled.[1] The anti-METH pAb generated by the MCV also appeared to have limited effects on concentrations of the active METH metabolite, AMP, in the serum and brain. This is not a disadvantage since humans produce substantially less of this metabolite than rats,[27,28] and even in rats antibody binding of these metabolites has not been shown to produce additional anti-METH effects.[23]

The combination treatment showed no indication that it was unsafe. There was no difference between the treatment groups (Figure 6) in terms of changes in bodyweight, temperature, or organ weight (determined at week 17). The gross pathology of the organs showed no differences or apparent abnormalities in the groups. All three groups gained similar amounts of weight over the course of the study. These male rat weight gains were similar to the values found in a previous study from our laboratory using a MCV and an activated-IC_{KLH} vehicle control group (without a METH-like hapten).[3] While there were similar slight temperature increases in all three groups early in the studies, the early temperature data from the mAb7F9-treated group functioned as an untreated control group prior to the administration of mAb on week 6. The average temperature of this group before mAb7F9 treatment was elevated by ~1°C on week 5 and was not significantly different from those of the also elevated IC_{KLH}- SOO9 or IC_{KLH}-SOO9 + mAb7F9 combination treated rats at this time point. Also, there were no temperature changes associated with any specific treatment time, and the temperature was not associated with any weight loss or changes in major organ systems. Therefore we do not think the one degree temperature change was a substantive finding.

Combination therapies effectively treat chronic conditions including hypertension,[29] asthma,[30] diabetes,[31] HIV infection,[32] or cancer.[33,34] Several preclinical studies have successfully combined mAb and vaccine treatments. For example, mAb therapy is used as an adjuvant to improve active immune responses by inhibiting immune system regulators[35,36] or by facilitating immune system interaction with an antigen.[37,38] Vaccine and mAb combinations can simultaneously perform different therapeutic actions.[39–41] Also, an antigen can be linked to a mAb to target an active immune response to a tumor.[42] However, after an extensive literature search, the current combined anti-METH mAb-MCV studies were found to be the first to report using an anti-METH mAb as a loading dose that provides an early boost to developing an active anti-METH pAb humoral response.

Researchers have successfully combined anti-nicotine mAb and vaccination therapy in preclinical studies, but in these studies, anti-drug mAb was administered at least 10 days after the vaccination regimen was completed.[11–13] Since the vaccine was administered before the mAb and there was a long separation in time between the vaccine and mAb regimens in these cocaine and nicotine studies, there is likely a low risk of the mAb inhibiting the active humoral response or resulting in an immunogenic reaction. While the approach by these previous investigations allows a mAb supplementation of the active humoral response (as our study also demonstrates), it does not provide early protection and initiation of the therapeutic benefits. The early protection presented in the current study would be important for addicted patients who badly need protection from METH effects before the active immune response titers and affinity reach peak effects.

Using a monoclonal antibody and polyclonal antibodies from a MCV vaccine against the same hapten target could potentially result in an inhibition of the active antibody response[17] and possibly lead to severe allergic reactions.[14,15] Our combination strategy likely avoided similar immune response inhibition or adverse effects by limiting antibody-vaccine interactions through careful hapten design and careful selection of the mAb for use in the combination treatment. In future studies, it would be important to confirm that the mAb7F9

could be dosed before the first vaccination with MCV without inhibiting the long-term immune response.

Summary

In conclusion, combined MCV-mAb7F9 therapy safely (Figure 6) led to early high concentrations of anti-METH antibodies due to the important contribution of mAb7F9 without hindering delayed yet long lasting IC_{KLH}-SOO9 induced active pAb immune response (Figures 2 and 4) and without hindering METH binding in the serum to decrease brain concentrations (Figure 5). Considering the similarity of therapeutic vaccine administration regimens used in humans and in this study[7,8] and the longer elimination $t_{1/2}$ of mAbs in humans,[43] an anti-METH mAb administered early during a vaccination regimen could provide protection during the development of the peak active pAb effects. In addition, anti-METH mAb therapy could be used as an adjunct treatment during active vaccination regimens in patients that are low responders to a MCV.

Experimental Section

General

^{1}H NMR spectra were determined on a Bruker 300 spectometer using tetramethylsilane as an internal standard. All reactions were followed by thin-layer chromatography using Whatman silica gel 60 TLC plates and were visualized by UV. Optical rotations were measured on an Auto Pol III polarimeter. All solvents were reagent grade. HCl in dry diethyl ether was purchased from Altech Chemical Co. and used while fresh before discoloration. CMA80 is a mixture of 80% chloroform, 18% methanol, and 2% concentrated ammonium hydroxide. Purity of compounds (>95%) was established by elemental analysis. Elemental analyses were performed by Atlantic Microlab, Inc., Atlanta, GA. (+)-METH HCl and [^{3}H]-METH were obtained from the National Institute on Drug Abuse drug supply program (Rockville, MD). (+)-METH HCl was prepared in 0.9% sterile saline at a concentration of 0.56 mg/ml free base. The liquid chromatography with tandem mass spectrometry (LC-MS/MS) standards (±)-METH and (±)-AMP as well as the internal standard (±)-1-Phenyl-1,2-dideutero-2-[trideuteromethyl]aminopropane (METH-d_5) were purchased from Cerilliant (Round Rock, TX). All other reagents and supplies were purchased from Sigma Chemical Company (St. Louis, MO) or Thermo-Fisher Scientific (Rockford, IL), unless noted.

(*S*,*S*)-*N*-α-Methylbenzyl-2-methoxyamphetamine (3) Hydrochloride

2-Methoxyacetophenone (**1**, 44.7 g, 0.272 mole) and (S)-(-)-a-methylbenzylamine (**2**, 34.0 g, 0.276 mol) were dissolved in ClCH$_2$CH$_2$Cl (2 L) and sodium triacetoxyborohydride (93.1 g, 0.426 mol) was added in five portions. The reaction mixture was stirred at room temperature for 16 h then added to 1 L of 25% NH$_4$OH. The mixture was stirred for 15 minutes, followed by separation of the organic layer. The organic layer was washed with brine, separated, dried (Na$_2$SO$_4$) and concentrated to give 72.2 g of colorless oil: ^{1}H NMR (free base, 300 MHz, MeOD) δ 7.27 (m, 3H), 7.18 (m, 2H), 7.02 (dd, *J* = 7.4, 1.8 Hz, 1H), 6.78 (m, 2H), 3.90 (t, *J* = 7.0 Hz, 1H), 3.68 (s, 3H), 2.96 (dd, *J* = 12.7, 5.0 Hz, 1H), 2.76 (m, 1H),

2.41 (dd, J = 12.8, 7.8 Hz, 1H), 1.56 (bs, 1H), 1.25 (d, J = 6.8 Hz, 3H), 0.87 (d, J = 6.4 Hz, 3H). Anal. $C_{18}H_{24}ClNO$) C, H, N.

The free base was dissolved in ether and acidified with 2M ethereal HCl (200 mL). After 30 minutes, the resulting solids were separated by filtration and dried to give 79.8 g (mp 200–202 °C). The solids were recrystallized three times from toluene to afford 32.8 g (40%) of diastereomerically pure **3** HCl; mp = 213–214 °C.

(*S,S*)-*N*-Formyl-*N*-α-methylbenzyl-2-methoxyamphethamine (4)

Acetic anhydride (85.7 g, 0.84 mol) in toluene (150 mL) was added to an ice cooled solution of 96% formic acid (53.8 g, 1.17 mol). After addition the mixture was stirred for 10 minutes then **3** (27.8 g, 0.1013 mol) in HCO_2H (50 mL) was added and the mixture was stirred at reflux for 18 h. The reaction mixture was cooled and stirred an additional 2 h at RT. The mixture was added to NH_4OH/H_2O (1:1, 600 mL), stirred and extracted with EtOAc. The organic layer was separated, dried (Na_2SO_4) and concentrated to afford an oil which was chromatographed on silica gel, eluting with EtOAc, to yield 6.40 g (38%) of **4** as a light yellow oil: ^{1}H NMR (300 MHz, $CDCl_3$) δ 8.35 (s, 1H), 8.22 (s, 1H), 7.02–7.21 (m, 8H), 7.02–7.08 (m, 2H), 6.91–7.02 (m, 2H), 6.81 (dd, J = 7.2, 1.5 Hz, 1H), 6.66 (d, J = 7.2 Hz, 1H), 6.59 (m, 1H), 6.53 (dd, J = 8.3, 5.3 Hz, 2H), 6.47 (dd, J = 7.2, 1.5 Hz, 1H), 5.64 (q, J = 7.2 Hz, 1H), 4.33 (q, J = 7.2 Hz, 1H), 3.56 (m, 1H), 3.48 (s, 3H), 3.44 (s, 3H), 3.26–3.41 (m, 1H), 2.91 (dd, J = 12.8, 8.3 Hz, 1H), 2.74 (dd, J = 12.8, 6.8 Hz, 1H), 2.58 (dd, J = 12.8, 9.4 Hz, 1H), 2.39 (dd, J = 12.8, 5.6 Hz, 1H), 1.39 (d, J = 7.2 Hz, 3H), 1.38 (d, J = 7.2 Hz, 3H), 1.15 (d, J = 6.8 Hz, 3H). Anal. ($C_{19}H_{23}NO_2$) C, H, N.

(*S*)-1-(2-Methoxyphenyl)-*N*-methyl*)*-*N*-((*S*)-1-phenylethyl)propan-2-amine (5)

To an ice cooled solution of compound **4** (12.0 g, 0.0404 mol) in THF (100 mL), 121 mL (0.121 mol) of 1M BH_3 in THF was added. After addition the reaction mixture was stirred at ambient temperature for 19 h. The reaction mixture was quenched with the careful addition of MeOH, then concentrated in vacuo to give an oil. The oil was chromatographed on silica gel, eluting with EtOAc, to afford 6.64 g (58%)of **5** as a clear oil: ^{1}H NMR (300 MHz, $CDCl_3$) δ 7.15–7.40 (m, 6H), 7.04 (m, 1H), 6.82 (m, 2H), 3.74 (s, 3H), 3.78 (m, 1H), 3.17 (bm, 1H), 2.95 (dd, J = 12.5, 6.6 Hz, 1H), 2.52 (m, 1H), 2.32 (s, 3H), 1.32 (d, J = 7.6 Hz, 3H), 0.92 (d, J = 7.8 Hz, 3H). Anal. ($C_{19}H_{25}NO$) C, H, N.

(*S*)-1-(2-Methoxyphenyl)-*N*-methylpropan-2-amine (6)

Compound **5** (6.64 g, 0.0234 mol) was dissolved in MeOH (200 mL) and ammonium formate (7.43 g, 0.118 mol) was added followed by 5% Pd/C (0.80 g). The reaction mixture was stirred and warmed to 50 °C and kept there for 4 h. The mixture was cooled, filtered through a pad of celite, washed with MeOH and concentrated in vacuo. The resulting oil was dissolved in CH_2Cl_2, filtered and concentrated to give an oil which was chromatographed on silica gel, eluting with 50CMA80/EtOAc, to yield 3.24 g (77%) of **6** as a yellow oil: $[a]^{22}_D$ +7.4 (c = 0.645, MeOH). ^{1}H NMR (300 MHz, $CDCl_3$) δ 7.10–7.27 (m, 2H), 6.82–6.93 (m, 2H), 3.82 (s, 3H), 2.95–3.10 (m, 2H), 2.60–2.70 (m, 1H), 2.54 (s, 3H), 1.17 (d, J = 6.5 Hz, 3H). Anal. ($C_{11}H_{17}NO$) C, H.

(*S*)-2-(2-Methylamino)propyl)phenol (7)

BBr$_3$ (18.8 g, 0.075 mol) in CH$_2$Cl$_2$ (20 mL) was added to compound **6** (4.05 g, 0.0226 mol) in CH$_2$Cl$_2$ (100 mL) that was chilled with an acetone dry ice bath. After addition the reaction mixture was stirred for 18 h, allowing the bath to come to RT. The mixture was cooled in an ice bath and excess BBr$_3$ was destroyed by the careful addition of MeOH. The mixture was concentrated in vacuo and MeOH was repeatedly (3X) added and concentrated. The resulting residue was chromatographed on silica gel, eluting with CMA80, to yield 2.60 g (70%) of **7** as a thick orange oi: ^{1}H NMR (300 MHz, MeOD) δ 7.09–7.16 (m, 2H), 6.77–6.86 (m, 2H), 3.50–3.60 (m, 1H), 3.09 (dd, *J* = 14.9, 8.5 Hz, 1H), 2.84 (dd, *J* = 13.3, 5.3 Hz, 1H), 2.73 (s, 3H), 1.27 (d, *J* = 6.6 Hz, 3H). This material was used in the next step without further purification.

(*S*)-*tert*-Butyl 1-(2-Hydroxyphenyl)propan-2-yl(methyl)carbamate (8)

To MeOH (30 mL) was added **7** (2.60 g, 0.0157 mol), Boc$_2$O (4.45 g, 0.0204 mol) and Et$_3$N (8.0 g, 0.079 mol). The reaction mixture was stirred at 50 °C for 2.5 h, concentrated and the residue was dissolved in EtOAc. The EtOAc was washed with H$_2$O followed by 10% NaHCO$_3$ and brine. The organic layer was separated, dried (Na$_2$SO$_4$) and concentrated in vacuo to yield 2.88 g (69%) of **8** as an orange oil which solidified upon standing: ^{1}H NMR (300 MHz, MeOD) δ 7.09 (bt, 1H), 7.00 (bd, 1H), 6.89 (bm, *J* = 6.0 Hz, 1H), 6.80 (t, *J* = 6.0 Hz, 1H), 4.14 (bs, 1H), 2.86 (bd, 1H), 2.81 (s, 3H), 2.28 (bm, 1H), 1.44 (bs, 9H), 1.18 (d, *J* = 6.7 Hz, 3H). Anal. (C$_{15}$H$_{23}$NO$_3$) C, H, N.

(*S*)-Methyl 5-(2-(2-*tert*-Butycarbonyl(methyl)amino-propyl)phenoxyl)hexanoate (9)

Compound **8** (2.88 g, 0.0109 mol) in DMF (20 mL) was added to 60% NaH (0.52 g, 0.0110 mol) in DMF (20 mL). The mixture was stirred for 30 minutes at RT then methyl 6-bromohexanoate (3.40 g, 0.0159 mol) in DMF (10 mL) was added. The reaction mixture was stirred at RT for 67 h then added to 300 mL of ice water. The mixture was stirred for 10 minutes, extracted with EtOAc, dried (Na$_2$SO$_4$) and concentrated to give 3.54 g (83%) of **9** as a thick orange oil: ^{1}H NMR (300 MHz, CDCl$_3$) δ 6.90–7.10 (m, 2H), 6.77–6.80 (m, 2H), 3.90 (t, *J* = 7.4 Hz, 2H), 3.60 (s, 3H), 2.51–2.72 (bm, 6H), 2.30 (t, *J* = 6.3 Hz, 2H), 1.35–1.82 (m, 6H), 1.00–1.36 (bm, 12H). This material was used in the next step without further purification.

(*S*)-5-(3-(2-(*tert*-Butoxycarbonyl(methyl)amino)propyl)-phenoxyl)hexanoic Acid (10)

Compound **9** (3.54 g, 0.0089 mol) in THF (45 mL) was added dropwise to LiOH (0.65 g, 0.0270 mol) in H$_2$O (15 mL). The reaction mixture was stirred at reflux for 3 h, then concentrated in vacuo to a thick gel. Water (100 mL) was added to the residue followed by 1$\underline{N}$ HCl until a pH of 7 was obtained. The mixture was extracted with CH$_2$Cl$_2$ to afford 3.00 g of a light yellow oil. The oil was chromatographed on silica gel, eluting with 50 hexane/EtOAc, to afford 2.0 g (59%) of **10** as a light yellow oil: [a]^{22}$_D$ = +53.4 (c = 0.545, MeOH). ^{1}H NMR (300 MHz, CDCl$_3$) δ 7.07 (m, 1H), 6.98 (bd, 1H), 6.71–6.79 (m, 2H), 3.91 (t, *J* = 6.3 Hz, 2H), 2.55–2.75 (bm, 6H), 2.33 (t, *J* = 7.6 Hz, 2H), 1.68–1.90 (m, 4H), 1.50–1.65 (m, 2H), 1.28 (bs, 9H), 1.10 (d, *J* = 6.8 Hz, 3H). Anal. (C$_{21}$H$_{33}$NO$_5$) C, H, N.

tert-Butylcarbonyl protected-METH-SSOO9 (11)

To THF (100 mL) was added **10** (1.96 g, 0.00516 mol), cystamine dihydrochloride (0.58 g, 0.00258 mol), BOP (2.28 g, 0.00282 mol) and Et$_3$N (3.14 g, 0.0311 mol). The mixture was stirred at RT under N$_2$ for 20 h. The mixture was concentrated in vacuo and ether was added to the residue. The mixture was washed with H$_2$O (3X), 10% NaHCO$_3$ (3X) and brine (3X). The organic layer was separated, dried (Na$_2$SO$_4$) and concentrated to yield 1.95 g (86%) of **11** as yellow-orange oil: ^{1}H NMR (300 MHz, CDCl$_3$) δ 7.02–7.19 (m, 2H), 6.77–6.87 (m, 2H), 3.95 (t, J = 6.3 Hz, 2H), 3.55 (bm, 2H), 2.73 (t, J = 7.0 Hz, 2H), 2.65–2.77 (m, 6H), 2.28 (t, J = 6.7 Hz, 2H), 1.67–1.90 (m, 2H), 1.45–1.60 (m, 1H), 1.08–1.40 (bm, 15H). This material was used in the next step without further purification.

(*S,S*)-6-{2-[2-(methylamino)propyl]phenoxyl}-N-(2-{[2-6-{2-[2-(methylamino)propyl]phenoxy}hexanamido)ethyl]disulfanyl}ethyl)hexanamide dihydrochloride (12) (METH-SSOO9)

2$\underline{M}$ Ethereal HCl (0.016 mol, 8 mL) was added to compound **11** (1.95 g, 0.00223 mol) in ether (100 mL). The reaction mixture was stirred at room temperature for 21 h. Solvent was decanted and the solids were washed with ether (keeping solids in the flask). The white solid was dried under high vacuum for 48 h to yield 1.78 g (99%) of **12** (**SSOO9**) as a beige solid: mp = 55–60 °C. R$_f$ = 0.52, silica gel, 75 CMA80/CH$_2$Cl$_2$. [a]$_D$ -3.5 (c = 0.695, MeOH). ^{1}H NMR (300 MHz, MeOD, salt) δ 7.25 (t, J = 5.4 Hz, 1H), 7.20 (m, 1H), 6.76–7.02 (m, 2H), 4.06 (t, J = 6.7 Hz, 2H), 3.50 (m, 4H), 3.10 (dd, J = 9.2, 4.5 Hz, 1H), 2.83 (m, 2H), 2.74 (s, 3H), 2.23 (t, J = 7.8 Hz, 2H), 1.86 (m, 2H), 1.72 (m, 2H), 1.55 (m, 2H), 1.20 (m, 3H). Anal. (C$_{36}$H$_{60}$Cl$_2$O$_4$N$_4$S$_2$ 2.0 H$_2$O) C, H, N.

tert-Butylcarbonylprotected-METH-SSMO9 (14)

To DMF (10 ml) was added **13** (1.15 g, 0.00304 mol), cystamine dihydrochloride (0.34 g, 0.00152 mol), EDC•HCl (0.583 g, 0.00304 mol) and Et$_3$N (1.54 g, 0.0152 mol). The mixture was stirred at RT under N$_2$ for 20 h, then at 70 °C for 2 h. The mixture was cooled to RT, added to water (200 ml), and extracted with EtOAc. The mixture was washed with H$_2$O (3X), 10% NaHCO$_3$ (3X) and brine (3X). The organic layer was separated, dried (Na$_2$SO$_4$) and concentrated to yield 0.734 g (55%) of **14** as a clear thick oil: ^{1}H NMR (300 MHz, CDCl$_3$) δ 7.10 (t, J = 8.1 Hz, 1H), 6.60–6.70 (bm, 3H), 3.86 (t, J = 6.2 Hz, 2H), 3.55 (bq, 2H), 2.82 (t, J = 6.5 Hz, 2H), 2.47–2.80 (bm, 6H), 2.26 (t, J = 8.7 Hz, 2H), 1.65–1.85 (m, 4H), 1.50 (m, 2H), 1.20–1.40 (bm, 9H), 1.07 (bs, 3H).

(*S,S*)-6-{3-[2-(methylamino)propyl]phenoxyl}-N-(2-{[2-6-{3-[2-(methylamino)propyl]phenoxy}hexanamido)ethyl]disulfanyl}ethyl)hexanamide Dihydrochloride (15) (METH-SSMO9)

2$\underline{M}$ Ethereal HCl (0.044 mol, 22 mL) was added to compound **14** (0.94 g, 0.00121 mol) in ether (30 mL). The reaction mixture was stirred at room temperature for 18 h. Solvent was decanted and the solids were washed with ether (keeping solids in the flask). The white solid was dried under high vacuum for 24 h. Upon exposure to air, solids quickly picked up moisture, isolated 0.82 g (78%) of **15** (**SSMO9**). R$_f$ = 0.37, silica gel, 75 CMA80/CH$_2$Cl$_2$. [α]$_D$ + 0.43 (c = 0.92, MeOH). ^{1}H NMR (300 MHz, MeOD, salt) δ 7.25 (t, J = 8.5 Hz, 1H),

6.83 (bm, 3H), 3.97 (t, J = 5.5 Hz, 2H), 3.49 (m, 4H), 3.10 (bdd, 3.0 Hz, 1H), 2.84 (t, J = 6.7 Hz, 2H), 2.74 (s, 3H), 2.23 (t, J = 8.1 Hz, 2H), 1.79 (m, 2H), 1.69 (m, 2H), 1.52 (m, 2H), 1.23 (d, J = 7.3 Hz, 3H). Anal. ($C_{36}H_{60}Cl_2O_4N_4S_2$ 1.5 H_2O) C, H, N.

MCV synthesis and preparation for administration and assays

To synthesize the IC_{KLH}-SOO9 MCV used for immunization, conjugation buffer (50 mM $NaPO_4$, 0.1 M EDTA, 0.9 M NaCl with 5% lactose, pH 7.5) was bubbled with argon (to remove oxygen) before the addition of IC_{KLH} (Biosyn Corp. Carlsbad, CA). Sulfo-SMCC in water was added to activate the IC_{KLH} protein. After the reaction was complete, a Zeba spin desalting column was used. The SSOO9 **(12)** hapten dimer precursor was reduced with 10 mM Tris(2-carboxyethyl)phosphine to produce the hapten monomer which was then added in a 50 mole excess to activated IC_{KLH} to produce the IC_{KLH}-SOO9 MCV (Figure 1A). The MCV was allowed to react with a 200 mole excess of cysteine to neutralize or end-cap any unconjugated IC_{KLH} sites. This prevented the possibility of unreacted hapten forming covalent bonds with proteins *in vivo*. The number of SOO9 haptens incorporated was determined by the radiometric method described by Peterson *et al.*[22] The final MCV product was then dialyzed into administration buffer (50 mM $NaPO_4$ with 5% lactose, pH 7.5) and frozen at −30°C until use. Before administration, the MCV was thawed, diluted in administration buffer, and mixed with Sigma Adjuvant System. The IC_{KLH}-SMO9 conjugation procedure is similar and is described in detail in the supplemental materials of Peterson *et al.*[22]

Conjugation of the haptens derived from SSOO9 and SSMO9 to the OVA carrier protein for enzyme-linked immunosorbent assay (ELISA) plate coating was identical to the synthesis of IC_{KLH}-SOO9 with some exceptions. No carrier protein activation was required prior to the conjugation due to use of Imject Maleimide Activated OVA. According to the manufacturer, this carrier protein contained 13 active sites per OVA molecule. A 30 mole excess of SOO9 or SMO9 hapten (monomer) was used for each conjugation. No end-cap reaction or adjuvant mixture was necessary since the products were not used *in vivo*. The number of SOO9/ SMO9 haptens incorporated was also determined as described for IC_{KLH}-SOO9.

MAb preparation

Synthesis of METH-like haptens, hapten conjugation to carrier protein, immunization of mice, and production of hybridoma cell lines are previously described.[6,25,44] Large scale production of anti-METH mAb, purification and formulation are described by Peterson *et al.*[44] MAb7F9 is an IgG1 isotype with a kappa light chain. It originates from mouse vaccination with a BSA carrier protein linked to the METH-MO9 hapten (see Figure 1A). The mAb7F9 K_d values for METH and AMP are 8 and 270 nM, respectively.[19,23] The $t_{1/2}$ in rats is estimated to be 7 days based on pharmacokinetic values for similar murine anti-METH mAb from our laboratory.[25]

MAb4G9 was produced with the MO9-(+)-METH hapten (see Figure 1A) linked to OVA. Anti-METH MAb4G9 was used only in the *in vitro* immunoassay experiment described below. It is a murine IgG2b isotype with a kappa light chain. Its K_d for METH = 16 nM and K_d for AMP = 110 nM.[23]

In vitro mAb and MCV interactions

The IC_{50} values for mAb binding to MCVs were generated by a modified radioimmunoassay (RIA) method, previously developed by our group.[25,44] Rather than measuring the METH inhibition of mAb7F9 or mAb4G9 binding to $[^3H]$-METH, this assay measured the MCV inhibition of mAb binding to $[^3H]$-METH. Each MCV, IC_{KLH}-SOO9 or IC_{KLH}-SMO9, was diluted 1:25–1:800. For each mAb, the ratio of RIA IC_{50} values of IC_{KLH}-SOO9 to IC_{KLH}-SMO9 was used to quantitate the immunological difference in mAb interaction between the two MCVs. This provided supportive evidence for choosing MAb7F9 for the in vivo combination experiments with the MCV.

Animals

Adult male Sprague-Dawley rats (*n*=24) were obtained from Charles River Laboratories (Raleigh, NC). The rats were housed two per cage and fed enough food pellets to maintain a 300–350 g body weight. Procedures involving pain or stress to the rats were conducted under isoflurane anesthesia with adequate depth of anesthesia determined by carefully monitoring respiration and the response to a paw pinch. All animal experiments were conducted with the approval of the Institutional Animal Care and Use Committee of the University of Arkansas for Medical Sciences and were in accordance with the Guide for the Care and Use of Laboratory Animals as adopted by the National Institutes of Health.

Immunization and mAb treatment

The 24 rats were weighed and distributed into two groups (n=8 and n=16) with the goal of these two groups having similar average weights. The n=8 group was the mAb7F9-only treatment group. Rats in the n=16 group were vaccinated with IC_{KLH}-SOO9 at time 0 and boosted at week 3 (see below for details on vaccination and analysis). The METH antibody binding titers were then measured in serum collected at week 5. These binding results were used to match-pair the animals into IC_{KLH}-SOO9-only and IC_{KLH}-SOO9 + mAb7F9 combination treatment groups. After final group assignment, all three groups were of similar average starting body weights (283 ± 15, 280 ± 14, and 278 ± 14 g).

In both the IC_{KLH}-SOO9-only and IC_{KLH}-SOO9 + mAb7F9 combination treatment groups, IC_{KLH}-SOO9 (100 μg) in Sigma Adjuvant System was administered *sc* into each hindquarter (50 μg each) at week 0. Booster immunizations occurred at weeks 3, 9, and 15. In both the mAb7F9-only and IC_{KLH}-SOO9 + mAb7F9 treatment groups, a 100 mg/kg dose of mAb7F9 was delivered intravenously (*iv*) on weeks 6 and 7 via the tail vein. MAb7F9-only treated rats were dosed *sc* with normal saline on MCV dosing days, and MCV-only treated rats were dosed *iv* with administration buffer on mAb dosing days. All rats (n=8 per group) completed the study.

Quantitation of combined anti-METH pAb and mAb7F9 $[^3H]$-METH binding

Blood samples were collected via the tail vein one day before and two weeks after each IC_{KLH}-SOO9 administration and one week after the second mAb7F9 dose. Rapid Equilibrium Dialysis (RED) cartridges and a $[^3H]$-METH tracer measured METH mAb and pAb binding in serum from the three groups. Each serum sample was diluted (1:50 and

1:300) with RED buffer (0.1 M NaPO$_4$, 0.15 M NaCl at pH 7.5) and a constant concentration of [^{3}H]-METH (5 nM). In anticipation of high METH binding, additional dilutions of 1:100, 1:1000, and/or 1:3000 were made depending on the proximity of sampling to mAb7F9 dosing. After loading 100 μl of diluted rat serum and [^{3}H]-METH to the cylindrical portion of the RED cartridge, 300 μl of RED buffer was added to the opposite side of the size exclusion membrane. The contents of the RED device were incubated overnight at 4°C to achieve equilibrium (determined in a prior experiment). Samples from each side of the membrane were collected and counted by liquid scintillation spectrophotometry to determine *in vitro* anti-METH antibody [^{3}H]-METH binding (*i.e.,* pAb and mAb contributions) as a percentage of total [^{3}H]-METH.

Analysis of individual anti-METH pAb or mAb7F9 binding by ELISA

Immulon HBX 96-well ELISA plates were coated with OVA-SOO9 or OVA-SMO9 (100 ng/well), blocked with superblock, and stored in a sealed container at 4°C until use. Serum samples from key time points (weeks 8, 11, and 17) were diluted in 10% Superblock ELISA wash buffer (PBS with 0.1% Tween 20) in half-log serial dilutions from 1:300 to 1:1,000,000. Duplicates of each sample dilution were plated in the ELISA wells. Samples from the three rat treatment groups were evenly distributed to the four ELISA plates (*i.e.*, two animals from each group per plate). Simultaneous analysis was conducted for each serum collection time point and repeated with each of the two hapten-protein conjugates (OVA-SOO9 for pAb detection and OVA-SMO9 for mAb7F9 detection). The contents of the microtiter plates were incubated overnight in a humid sealed container at 4°C. After washing the plates to remove unbound antibody, the bound anti-METH antibodies were detected by using appropriate species-specific secondary antibodies (Bethyl, Montgomery, TX). The OVA-SOO9 coated plates were treated with a diluted goat anti-rat IgG Fc-alkaline phosphatase conjugated antibody for detection of the active MCV-induced rat anti-METH antibodies. The OVA-SMO9 coated plates were treated with a diluted goat anti-mouse IgG Fc-alkaline phosphatase conjugated antibody for detection of mouse-derived mAb7F9. After incubation at room temperature, the plates were rinsed and then treated with p-nitrophenol. The absorbance in each well at 405 nm was determined with an Epoch Microplate Spectrophotometer and Gen5 data analysis software (BioTek, Winooski, VT). The four simultaneously analyzed plates were measured every 10 min until the UV absorbance reached a standardized value of 2.0 in any well, or for 1.5 hr of reaction time, whichever came first. For each time point, area under the absorbance vs time curve for all dilutions was used for comparisons of the presence of each antibody (rat or mouse). To further characterize the interaction between the SOO9-METH hapten and mAb7F9, the serum samples from week 8 (one week after the final mAb7F9 dose) were again analyzed on OVA-SOO9 coated plates but with the anti-mouse secondary antibody.

Determination of average affinity of pAb for METH

On week 17, these values in the serum pAb group were determined by a radioimmunoassay described previously.[3]

METH challenge doses and resulting serum and brain METH and AMP concentrations

Each rat was challenged with 0.56 mg/kg *sc* METH one day after the collection of blood samples for measurement of antibody titers on weeks 11 and 17. Two hrs after the first METH injection (week 11), blood samples were collected from the tail vein of rats under isoflurane anesthesia. Two hrs after the second METH challenge (week 17) at the end of the study, rats were euthanized under isoflurane anesthesia by decapitation for collection of brains and trunk blood. Serum was stored at −30°C. Brains were flash frozen in liquid nitrogen before being stored at −80°C.

For analysis of METH and AMP tissue concentrations, Strata X-C 33 µM Polymeric Strong Cation solid phase extraction columns (Phenomenex, Torrance, CA) were conditioned with 2 ml methanol and 2 ml extraction loading buffer (100 mM $NaPO_4$, pH 8.1). Before extraction of METH and AMP, brains were diluted in 4 ml liquid chromatography mass spectrometry (LCMS) grade water per gram of tissue and then homogenized. A METH and AMP standard curve in serum (0.3 to 2000 ng/ml) and quality control standards were prepared for analysis of serum and brain samples as previously described.[45] With each sample or standard, 25 µl aliquots were mixed with an equal volume of 0.2% formic acid. Afterward, one ml of loading buffer containing 2.5 ng/ml of the METH-d_5 internal standard was added. The mixture was transferred to the solid phase extraction column and rinsed with methanol. After drying the column, 5% NH_4OH, 5% tetrahydrofuran in acetonitrile was used to elute the METH and AMP into tubes containing 0.5 N HCl. The samples were then dried using nitrogen gas, reconstituted with 0.1% formic acid, and centrifuged to remove any precipitates.

The concentration of METH and AMP were determined using an Acquity Ultra Performance Liquid Chromatography system interfaced with a Quattro Premier XE mass spectrometer (Waters Corp, Milford, MA). Analytes were separated using a linear binary gradient with reversed-phase chromatography at a flow rate of 0.4 ml/min (mobile phase A: 0.1% formic acid; mobile phase B: 0.1% formic acid in acetonitrile). The gradient program was as follows: 0–1 min: 10% B; 1–4 min: 10% – 90% B and held for 1 min; 5–6 min: 90% - 10% B. The total run time was 7 min. Each sample (5 µl) was injected onto an Acquity UPLC BEH C18 1.7 µm (2.1 i.d. x 100 mm) column (Waters Corp). The column was maintained at 40°C and coupled to an electrospray ionization probe, which was operated in the positive ion mode.

Positive ions for AMP, METH, and METH-d_5, were generated at cone voltages of 18, 18, 21 volts, respectively. Product ions AMP, METH, and METH-d_5 were generated using argon collision induced disassociation at collision energy of 16, 15, and 21 eV while maintaining a collision cell pressure of 3×10^{-3} torr. Detection was achieved in the multiple-reaction-monitoring (MRM) mode using the precursor→product ions, *m/z* 135.8→90.8, 149.8→90.8, and 155.2→91.5 for AMP, METH, and METH-d_5, respectively. The lower and upper limit of quantification for METH and AMP was 1 and 1000 ng/ml, respectively. All predicted values for standards were within ± 20%.

Rat Safety measures

Rat weights were determined two to three times per week, and rectal temperatures were measured one to two times per week as general measures of health during immunization. The immunization sites and nine major organs (heart, lung, thymus, lymph nodes, liver, intestines, kidneys, adrenals, and spleen) were examined by a veterinary pathologist for possible adverse effects at the end of the study. The organ weights of the heart, liver, kidney, and spleen were also measured.

Statistical Analysis

RED [^{3}H]-METH binding, ELISA mAb or pAb binding AUC values, serum concentrations, body temperature, and body weight data were analyzed using two-way repeated measures analysis of variance (ANOVA) (day x treatment group), followed by Bonferroni Multiple Comparison tests. A one-way ANOVA with a post-hoc Bonferroni's test was used to compare brain concentrations and organ weights between the three groups on week 17. An unpaired student's t-test was used to compare week 17 average pAb affinities for METH between both groups receiving the IC$_{KLH}$-SOO9 vaccine. This statistical analysis was also used to compare week 17 serum and brain concentrations of the mAb7F9-only treated rats with our laboratory's historical control values from activated-KLH (without METH-like haptens) immunized rats to assure that the METH serum concentrations in the mAb7F9-treated group had returned to baseline. A paired student's t-test was used to compare RED [^{3}H]-METH binding in the mAb7F9 group on day 17 to pre-treatment baseline values to assure METH binding had returned to baseline. GraphPad Prism software (San Diego, CA) was used for all statistical analysis. Statistical significance was attained at p<0.05.

Supplementary Material

Refer to Web version on PubMed Central for supplementary material.

Acknowledgments

ABBREVIATIONS

AMP	amphetamine
ANOVA	analysis of variance
AUC	Area under the absorbance vs serum dilution curve
BSA	bovine serum albumin
DNP	dinitrophenyl

IC_{50}	half maximal inhibitory concentration
IC_{KLH}	Immunocyanin
KLH	keyhole limpet hemocyanin
LC-MS/MS	liquid chromatography with tandem mass spectrometry
METH	methamphetamine
MCV	METH conjugate vaccine
mAb	monoclonal antibody
OVA	ovalbumin
pAb	polyclonal antibody
RED	Rapid Equilibrium Dialysis
sulfo-SMCC	sulfosuccinimidyl-4-[N-maleimidomethyl]cyclohexane-1-carboxylate
SMO9	mercapto-hapten (S)-N-(2-(mercaptoethyl)-6-(3-(2-(methylamino)propyl)phenoxy)hexanamide
SOO9	mercapto-hapten (S)-N-(2-(mercaptoethyl)-6-(2-(2-(methylamino)propyl)phenoxy)hexanamide
SSMO9	(S,S)-6-{3-[2-(methylamino)propyl]phenoxyl}-N-(2-{[2-6-{3-[2-(methylamino)propyl]phenoxy}hexanamido)ethyl]disulfanyl}ethyl)hexanamide Dihydrochloride
SSOO9	(S,S)-6-{2-[2-(methylamino)propyl]phenoxyl}-N-(2-{[2-6-{2-[2-(methylamino)propyl]phenoxy}hexanamido)ethyl]disulfanyl}ethyl)hexanamide dihydrochloride

References

1. Hambuchen MD, Rüedi-Bettschen D, Williams DK, Hendrickson H, Owens SM. Treatment Of Rats With An Anti-(+)-Methamphetamine Monoclonal Antibody Shortens The Duration Of Action Of Repeated (+)-Methamphetamine Challenges Over A One Month Period. Vaccine. 2014; 32:6213–6219. [PubMed: 25252196]

2. Stevens MW, Henry RL, Owens SM, Schutz R, Gentry WB. First Human Study Of A Chimeric Anti-Methamphetamine Monoclonal Antibody In Healthy Volunteers. MAbs. 2014; 6:1649–1656. [PubMed: 25484042]

3. Rüedi-Bettschen D, Wood SL, Gunnell MG, West CM, Pidaparthi RR, Carroll FI, Blough BE, Owens SM. Vaccination Protects Rats From Methamphetamine-Induced Impairment Of Behavioral Responding For Food. Vaccine. 2013; 31:4596–4602. [PubMed: 23906885]

4. Brensilver M, Heinzerling KG, Shoptaw S. Pharmacotherapy Of Amphetamine-Type Stimulant Dependence: An Update. Drug Alcohol Rev. 2013; 32:449–460. [PubMed: 23617468]

5. Gentry WB, Rüedi-Bettschen D, Owens SM. Anti-(+)-Methamphetamine Monoclonal Antibody Antagonists Designed To Prevent The Progression Of Human Diseases Of Addiction. Clin Pharmacol Ther. 2010; 88:390–393. [PubMed: 20668443]

Author Manuscript

Author Manuscript

Author Manuscript

Author Manuscript

6. Owens SM, Atchley WT, Hambuchen MD, Peterson EC, Gentry WB. Monoclonal Antibodies As Pharmacokinetic Antagonists For The Treatment Of (+)-Methamphetamine Addiction. CNS Neurol Disord-Dr. 2011; 10:892–898.

7. Cornuz J, Zwahlen S, Jungi WF, Osterwalder J, Klingler K, van Melle G, Bangala Y, Guessous I, Müller P, Willers J, Maurer P, Bachmann MF, Cerny T. A Vaccine Against Nicotine For Smoking Cessation: A Randomized Controlled Trial. PloS one. 2008; 3:1–10.

8. Hatsukami DK, Jorenby DE, Gonzales D, Rigotti NA, Glover ED, Oncken CA, Tashkin DP, Reus VI, Akhavain RC, Fahim RE, Kessler PD, Niknian M, Kalnik MW, Rennard SI. Immunogenicity And Smoking-Cessation Outcomes For A Novel Nicotine Immunotherapeutic. Clin Pharmacol Ther. 2011; 89:392–399. [PubMed: 21270788]

9. Martell BA, Orson FM, Poling J, Mitchell E, Rossen RD, Gardner T, Kosten TR. Cocaine Vaccine For The Treatment Of Cocaine Dependence In Methadone-Maintained Patients: A Randomized, Double-Blind, Placebo-Controlled Efficacy Trial. Arch Gen Psychiat. 2009; 66:1116–1123. [PubMed: 19805702]

10. Tonstad S, Heggen E, Giljam H, Lagerbäck P, Tønnesen P, Wikingsson LD, Lindblom N, de Villiers S, Svensson TH, Fagerström K. Niccine®, A Nicotine Vaccine, For Relapse Prevention: A Phase II, Randomized, Placebo-Controlled, Multicenter Clinical Trial. Nicotine Tob Res. 2013; 15:1492–1501. [PubMed: 23471101]

11. Carrera MR, Ashley JA, Zhou B, Wirsching P, Koob GF, Janda KD. Cocaine Vaccines: Antibody Protection Against Relapse In A Rat Model. Proc Natl Acad Sci US A. 2000; 97:6202–6206.

12. Roiko SA, Harris AC, Keyler DE, Lesage MG, Zhang Y, Pentel PR. Combined Active And Passive Immunization Enhances The Efficacy Of Immunotherapy Against Nicotine In Rats. J Pharmacol Exp Ther. 2008; 325:985–993. [PubMed: 18305013]

13. Cornish KE, Harris AC, Lesage MG, Keyler DE, Burroughs D, Earley C, Pentel PR. Combined Active And Passive Immunization Against Nicotine: Minimizing Monoclonal Antibody Requirements Using A Target Antibody Concentration Strategy. Int Immunopharmacol. 2011; 11:1809–1815. [PubMed: 21802529]

14. Tsujimura Y, Obata K, Mukai K, Shindou H, Yoshida M, Nishikado H, Kawano Y, Minegishi Y, Shimizu T, Karasuyama H. Basophils Play A Pivotal Role In Immunoglobulin-G-Mediated But Not Immunoglobulin-E-Mediated Systemic Anaphylaxis. Immunity. 2008; 28:581–589. [PubMed: 18342553]

15. Jiao D, Liu Y, Lu X, Pan Q, Zheng J, Liu B, Wang Y, Fu N. Characteristics Of Anaphylaxis-Inducing Igg Immune Complexes Triggering Murine Passive Systemic Anaphylaxis. Allergy. 2013; 68:236–245. [PubMed: 23252369]

16. Caulfield MJ, Shaffer D. Immunoregulation By Antigen/Antibody Complexes. I. Specific Immunosuppression Induced In Vivo With Immune Complexes Formed In Antibody Excess. J Immunol. 1987; 138:3680–3683. [PubMed: 3584970]

17. Elazab MF, Fukushima Y, Horiuchi H, Matsuda H, Furusawa S. Prolonged Suppression Of Chick Humoral Immune Response By Antigen Specific Maternal Antibody. J Vet Med Sci. 2009; 71:417–424. [PubMed: 19420843]

18. Carroll FI, Abraham P, Gong PK, Pidaparthi RR, Blough BE, Che Y, Hampton A, Gunnell MG, Lay JO Jr, Peterson EC, Owens SM. The Synthesis Of Haptens And Their Use For The Development Of Monoclonal Antibodies For Treating Methamphetamine Abuse. J Med Chem. 2009; 52:7301–7309. [PubMed: 19877685]

19. Stevens MW, Tawney RL, West CM, Kight AD, Henry RL, Owens SM, Gentry WB. Preclinical Characterization Of An Anti-Methamphetamine Monoclonal Antibody For Human Use. MAbs. 2014; 6:547–555. [PubMed: 24492290]

20. Nichols DE, Barfknecht CF, Rusterholz DB, Benington F, Morin RD. Asymmetric Synthesis Of Psychotomimetic Phenylisopropylamines. J Med Chem. 1973; 16:480–483. [PubMed: 4718460]

21. Carroll FI, Blough BE, Pidaparthi RR, Abraham P, Gong PK, Deng L, Huang X, Gunnell MG, Lay JO Jr, Peterson EC, Owens SM. Synthesis Of Mercapto-(+)-Methamphetamine Haptens And Their Use For Obtaining Improved Epitope Density On (+)-Methamphetamine Conjugate Vaccines. J Med Chem. 2011; 54:5221–5228. [PubMed: 21682289]

22. Peterson EC, Hambuchen MD, Tawney RL, Gunnell MG, Cowell JL, Lay JO Jr, Blough BE, Carroll FI, Owens SM. Simple Radiometric Method For Accurately Quantitating Epitope Densities Of Hapten-Protein Conjugates With Sulfhydryl Linkages. Bioconjugate Chem. 2014; 25:2112–2115.

23. Laurenzana EM, Stevens MW, Frank JC, Hambuchen MD, Hendrickson HP, White SJ, Williams DK, Owens SM, Gentry WB. Pharmacological Effects Of Two Anti-Methamphetamine Monoclonal Antibodies: Supporting Data For Lead Candidate Selection For Clinical Development. Hum Vaccin Immunother. 2014; 10:2638–2647. [PubMed: 25483484]

24. Cho AK. Ice: A New Dosage Form Of An Old Drug. Science. 1990; 249:631–634. [PubMed: 17831955]

25. Laurenzana EM, Hendrickson HP, Carpenter D, Peterson EC, Gentry WB, West M, Che Y, Carroll FI, Owens SM. Functional And Biological Determinants Affecting The Duration Of Action And Efficacy Of Anti-(+)-Methamphetamine Monoclonal Antibodies In Rats. Vaccine. 2009; 27:7011–7020. [PubMed: 19800446]

26. Miller ML, Moreno AY, Aarde SM, Creehan KM, Vandewater SA, Vaillancourt BD, Wright MJ Jr, Janda KD, Taffe MA. A Methamphetamine Vaccine Attenuates Methamphetamine-Induced Disruptions In Thermoregulation And Activity In Rats. Biol Psychiat. 2013; 73:721–728. [PubMed: 23098894]

27. Cook CE, Jeffcoat AR, Hill JM, Pugh DE, Patetta PK, Sadler BM, White WR, Perez-Reyes M. Pharmacokinetics Of Methamphetamine Self-Administered To Human Subjects By Smoking S-(+)-Methamphetamine Hydrochloride. Drug Metab Dispos. 1993; 21:717–723. [PubMed: 8104133]

28. Rivière GJ, Byrnes-Blake KA, Gentry WB, Owens SM. Spontaneous Locomotor Activity And Pharmacokinetics Of Intravenous Methamphetamine And Its Metabolite Amphetamine In The Rat. J Pharmacol Exp Ther. 1999; 291:1220–1226. [PubMed: 10565845]

29. Chobanian AV, Bakris GL, Black HR, Cushman WC, Green LA, Izzo JL Jr, Jones DW, Materson BJ, Oparil S, Wright JT Jr, Roccella EJ. The Seventh Report Of The Joint National Committee On Prevention, Detection, Evaluation, And Treatment Of High Blood Pressure: The JNC 7 Report. JAMA. 2003; 289:2560–2572. [PubMed: 12748199]

30. EPR-3. Expert Panel Report 3 (EPR-3): Guidelines For The Diagnosis And Management Of Asthma-Summary Report 2007. 2007; 120(5 Suppl):S94–138.

31. Inzucchi SE, Bergenstal RM, Buse JB, Diamant M, Ferrannini E, Nauck M, Peters AL, Tsapas A, Wender R, Matthews DR. Management Of Hyperglycemia In Type 2 Diabetes: A Patient-Centered Approach: Position Statement Of The American Diabetes Association (ADA) And The European Association For The Study Of Diabetes (EASD). Diabetes Care. 2012; 35:1364–1379. [PubMed: 22517736]

32. Thompson MA, Aberg JA, Hoy JF, Telenti A, Benson C, Cahn P, Eron JJ, Günthard HF, Hammer SM, Reiss P, Richman DD, Rizzardini G, Thomas DL, Jacobsen DM, Volberding PA. Antiretroviral Treatment Of Adult HIV Infection: 2012 Recommendations Of The International Antiviral Society-USA Panel. JAMA. 2012; 308:387–402. [PubMed: 22820792]

33. Theriault RL, Carlson RW, Allred C, Anderson BO, Burstein HJ, Edge SB, Farrar WB, Forero A, Giordano SH, Goldstein LJ, Gradishar WJ, Hayes DF, Hudis CA, Isakoff SJ, Ljung BE, Mankoff DA, Marcom PK, Mayer IA, McCormick B, Pierce LJ, Reed EC, Schwartzberg LS, Smith ML, Soliman H, Somlo G, Ward JH, Wolff AC, Zellars R, Shead DA, Kumar R. Breast Cancer, Version 3. 2013. J Natl Compr Canc Netw. 2013; 11:753–761. [PubMed: 23847214]

34. Socinski MA, Evans T, Gettinger S, Hensing TA, Sequist LV, Ireland B, Stinchcombe TE. Treatment Of Stage IV Non-Small Cell Lung Cancer: Diagnosis And Management Of Lung Cancer, 3Rd Ed: American College Of Chest Physicians Evidence-Based Clinical Practice Guidelines. Chest. 2013; 143:e341S–368S. [PubMed: 23649446]

35. Tan C, Reddy V, Dannull J, Ding E, Nair SK, Tyler DS, Pruitt SK, Lee WT. Impact Of Anti-CD25 Monoclonal Antibody On Dendritic Cell-Tumor Fusion Vaccine Efficacy In A Murine Melanoma Model. J Transl Med. 2013; 11:1–9. [PubMed: 23281771]

36. Williams EL, Dunn SN, James S, Johnson PW, Cragg MS, Glennie MJ, Gray JC. Immunomodulatory Monoclonal Antibodies Combined With Peptide Vaccination Provide Potent

Immunotherapy In An Aggressive Murine Neuroblastoma Model. Clin Cancer Res. 2013; 19:3545–3555. [PubMed: 23649004]

37. Carlring J, Szabo MJ, Dickinson R, de Leenheer E, Heath AW. Conjugation Of Lymphoma Idiotype To CD40 Antibody Enhances Lymphoma Vaccine Immunogenicity And Antitumor Effects In Mice. Blood. 2012; 119:2056–2065. [PubMed: 22234700]

38. Kreutz M, Giquel B, Hu Q, Abuknesha R, Uematsu S, Akira S, Nestle FO, Diebold SS. Antibody-Antigen-Adjuvant Conjugates Enable Co-Delivery Of Antigen And Adjuvant To Dendritic Cells In Cis But Only Have Partial Targeting Specificity. PloS one. 2012; 7:1–12.

39. Orlandi F, Guevara-Patiño JA, Merghoub T, Wolchok JD, Houghton AN, Gregor PD. Combination Of Epitope-Optimized DNA Vaccination And Passive Infusion Of Monoclonal Antibody Against HER2/Neu Leads To Breast Tumor Regression In Mice. Vaccine. 2011; 29:3646–3654. [PubMed: 21435405]

40. Manzur S, Cohen S, Haimovich J, Hollander N. Enhanced Therapeutic Effect Of B Cell-Depleting Anti-CD20 Antibodies Upon Combination With In-Situ Dendritic Cell Vaccination In Advanced Lymphoma. Clin Exp immunol. 2012; 170:291–299. [PubMed: 23121670]

41. Ly LV, Sluijter M, van der Burg SH, Jager MJ, van Hall T. Effective Cooperation Of Monoclonal Antibody And Peptide Vaccine For The Treatment Of Mouse Melanoma. J Immunol. 2013; 190:489–496. [PubMed: 23203930]

42. Klier U, Maletzki C, Kreikemeyer B, Klar E, Linnebacher M. Combining Bacterial-Immunotherapy With Therapeutic Antibodies: A Novel Therapeutic Concept. Vaccine. 2012; 30:2786–2794. [PubMed: 22342917]

43. Wang W, Wang EQ, Balthasar JP. Monoclonal Antibody Pharmacokinetics And Pharmacodynamics. Clin Pharmacol Ther. 2008; 84:548–558. [PubMed: 18784655]

44. Peterson EC, Gunnell MG, Che Y, Goforth RL, Carroll FI, Henry R, Liu H, Owens SM. Using Hapten Design To Discover Therapeutic Monoclonal Antibodies For Treating Methamphetamine Abuse. J Pharmacol Exp Ther. 2007; 322:30–39. [PubMed: 17452421]

45. Hendrickson H, Laurenzana EM, Owens SM. Quantitative Determination Of Total Methamphetamine And Active Metabolites In Rat Tissue By Liquid Chromatography With Tandem Mass Spectrometric Detection. AAPS J. 2006; 8:E709–717. [PubMed: 17233534]

Biography

S. Michael Owens is Chief Scientific Officer and has financial interests in InterveXion Therapeutics, LLC, a pharmaceutical biotech company, whose main interest is the development of antibody medications for the treatment of human diseases, including drug abuse.
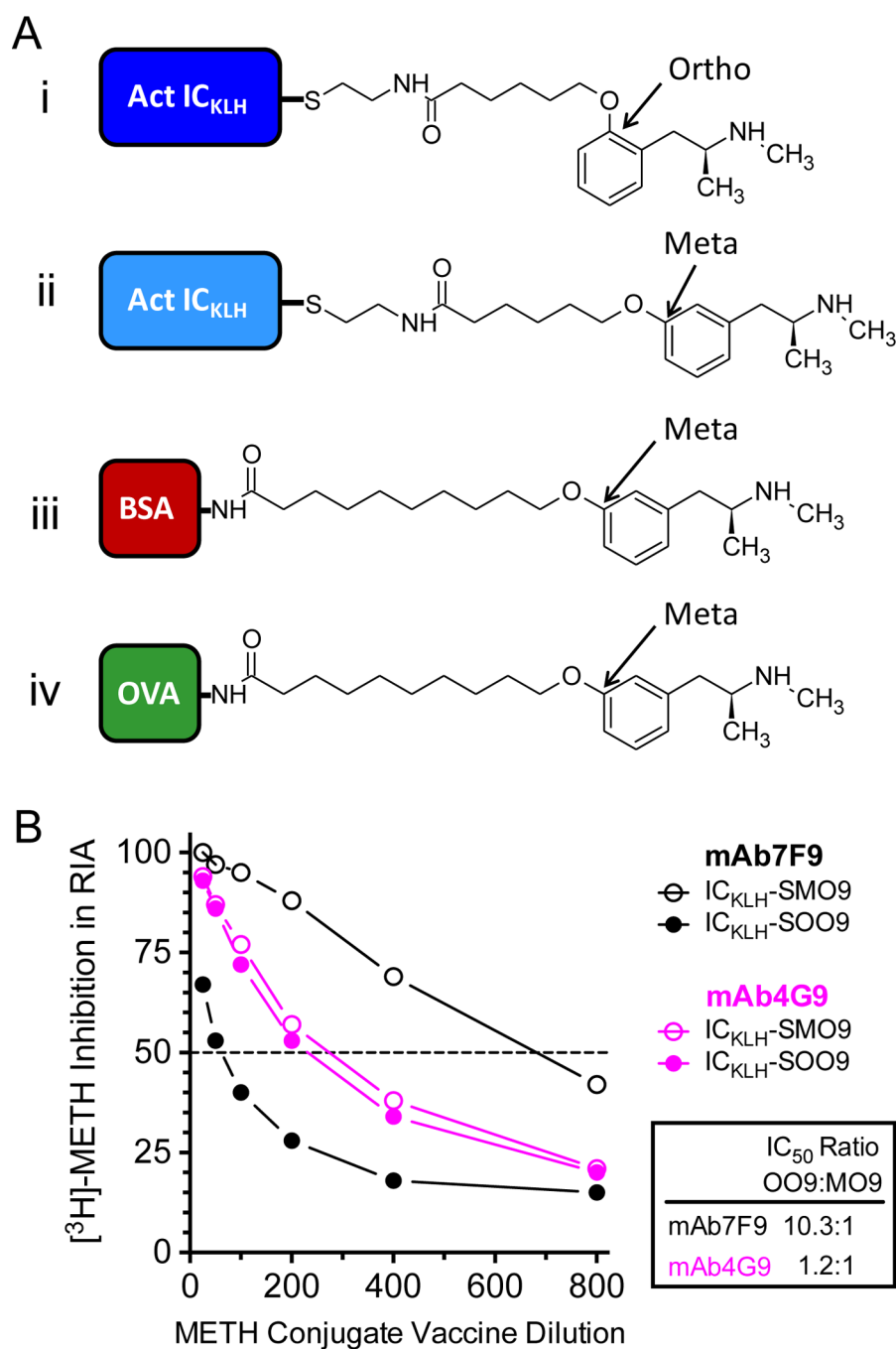
Figure 1.

(A) The MCV used for active immunization (IC_{KLH}-SOO9; i.), the other MCV tested *in vitro* (IC_{KLH}-SOO9; ii.), the MCV used to generate mAb7F9 (BSA-MO9; iii.), and the MCV used to generate mAb4G9 (OVA-MO9; iv.). (B) *In vitro* percent inhibition of mAb7F9 or mAb4G9 [³H]-METH binding by IC_{KLH}-SOO9 (i.) or IC_{KLH}-SMO9 (ii.) MCVs. These data aided the decision to use IC_{KLH}-SOO9 and mAb7F9 for these studies, since this combination showed the least cross reactivity.
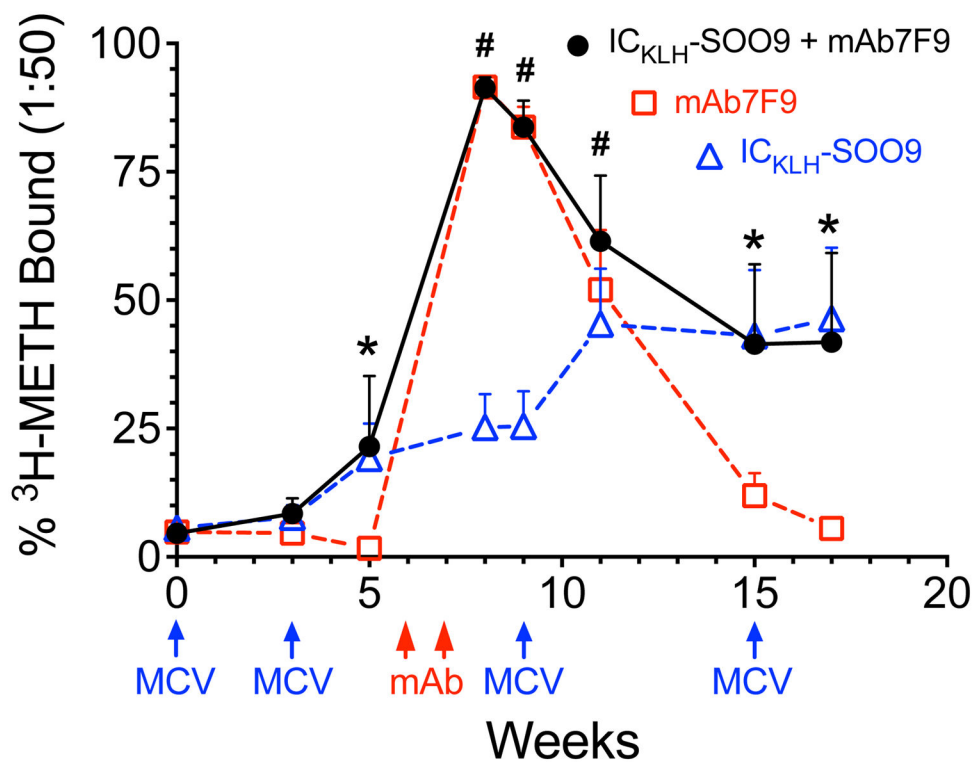
Figure 2.
Total anti-METH antibody (mAb7F9 and/or polyclonal) binding shown as the percentage [^{3}H]-METH bound by a 1:50 diluted rat serum sample over time. Dosing times and immunological treatments are denoted below the x-axis (combination treated rats were administered all MCV and mAb treatments). Statistical differences between METH binding in IC_{KLH}-SOO9 + mAb7F9, mAb7F9-only, and IC_{KLH}-SOO9-only treated animals were determined with a two-way repeated measures ANOVA with a post-hoc Bonferroni's test. For clarity, only statistical analysis comparing IC_{KLH}-SOO9 + mAb7F9 combination group with the other two treatment groups are shown. The * symbol denotes statistical significance compared to mAb7F9 treated animals, and the # symbol denotes statistical significance compared to IC_{KLH}-SOO9 treated animals ($p<0.05$).
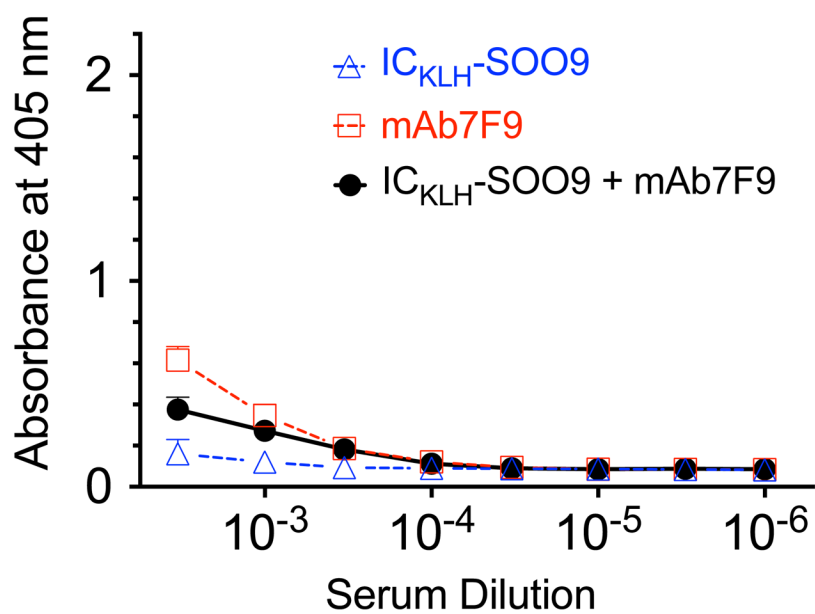
Figure 3.
Data from the ELISA determination of immune binding of mAb7F9 in rat serum (week 8) to microtiter plates coated with OVA-SOO9, followed by detection with an anti-mouse secondary antibody.
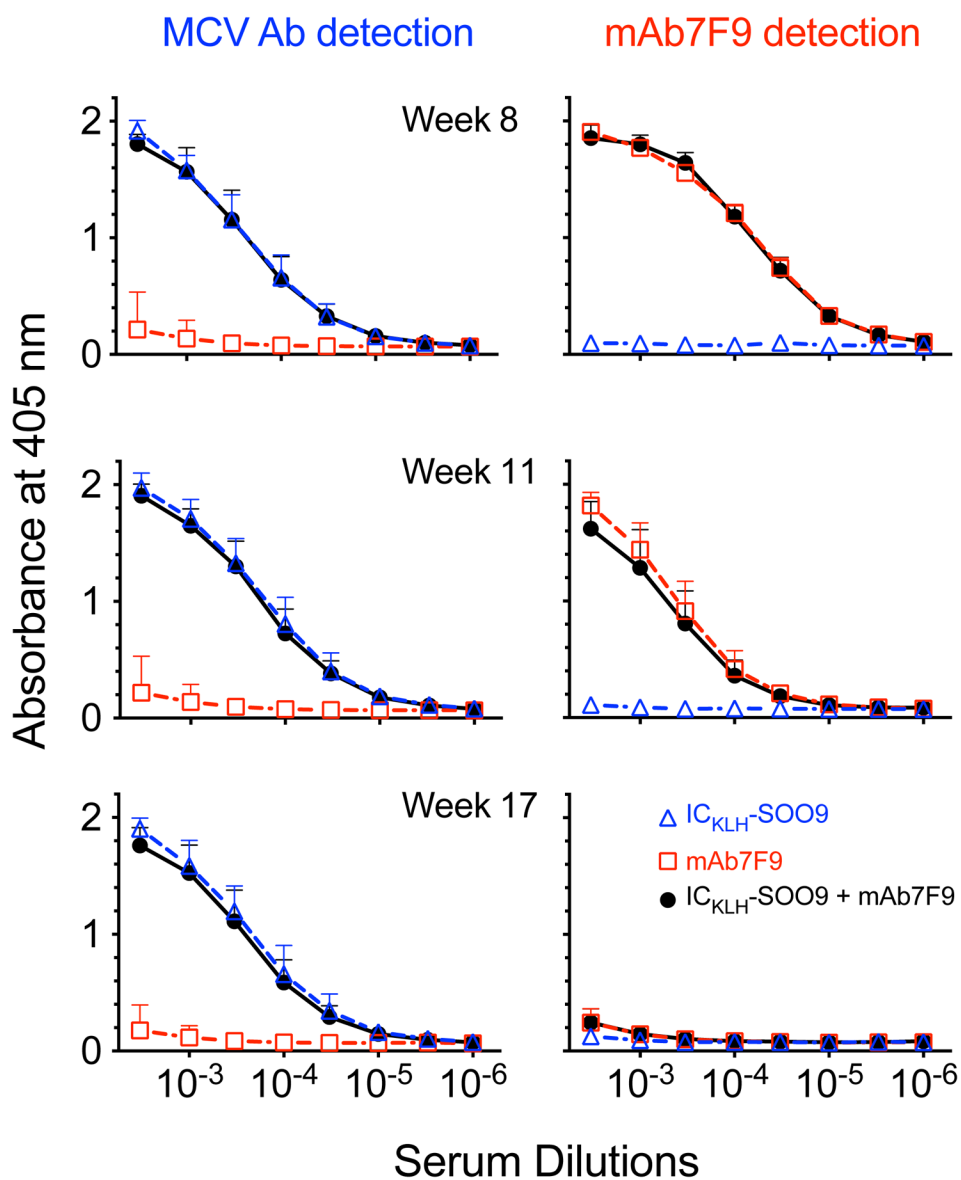
Figure 4.
Analysis of serum samples by ELISA for the presence of anti-METH pAb and mAb7F9 antibodies. Figures in the left panel show presence of anti-METH rat pAb over time (OVA-SOO9 ELISA plate coating, detection with anti-rat secondary Ab). Figures in the right panel show presence of mouse anti-METH mAb7F9 over time (OVA-SMO9 ELISA plate coating, detection with anti-mouse secondary Ab). See statistical comparisons in the results section.
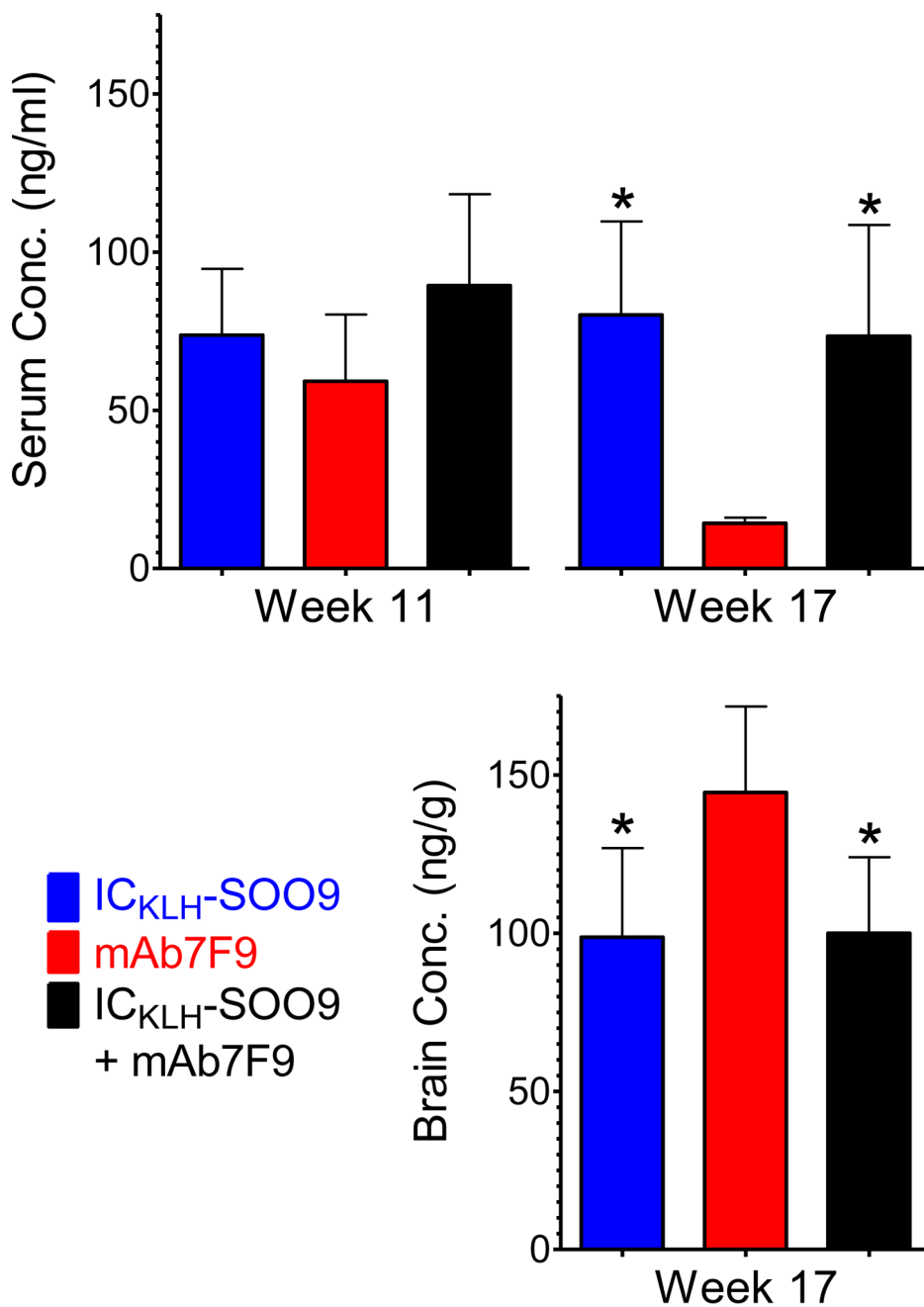
Figure 5.
METH serum and brain concentrations 2 hrs after a 0.56 mg/kg *sc* METH dose. The *
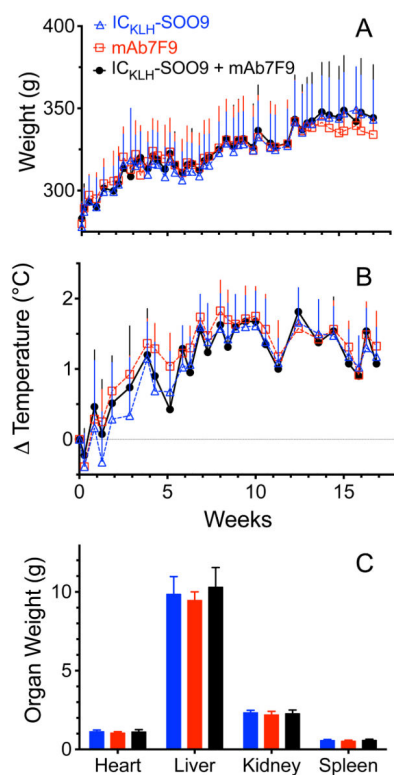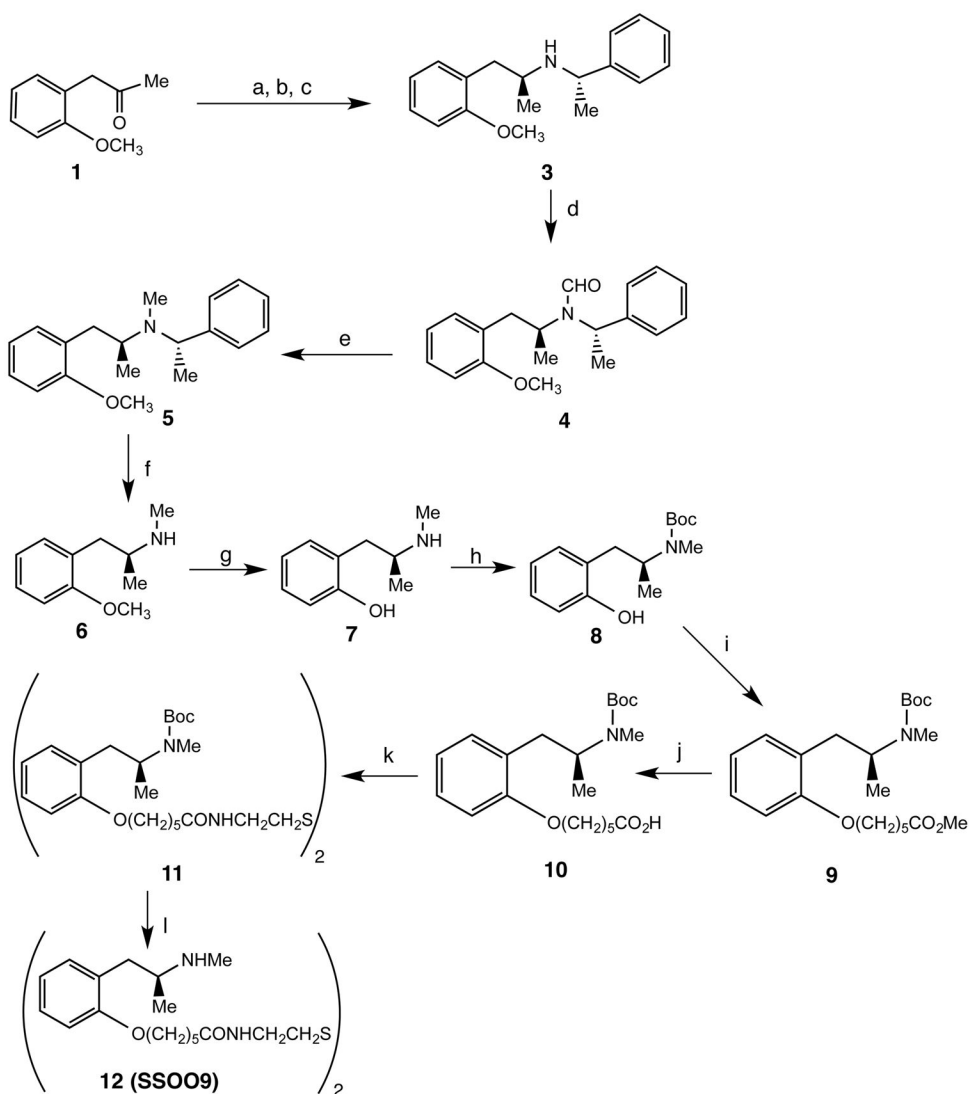denotes statistical significance compared to mAb7F9 treated animals (p<0.05).

Figure 6.
(A) Average animal weight per group (n=8 rats) over time (upper panel). (B) Change in average body temperature per group over time compared to baseline values (lower panel). (C) Average organ weights per group determined at the end of the studies.

Scheme 1[a]

[a]Reagents: (a) (*S*)-2-methylbenzlamine (**2**), Na(OAc)$_3$BH$_3$, (CH$_2$Cl)$_2$; (b) etheral HCl; (c) recrystallization from toluene; (d) HCO$_2$H, (CH$_3$CO)$_2$O, toluene; (e) BH$_3$, THF; (f) HCO$_2$NH$_4$, 5% Pd/C, CH$_3$OH; (g) BBr$_3$, CH$_2$Cl$_2$; (h) (BOC)$_2$O, Et$_3$N, CH$_3$OH; (i) NaH, Br(CH$_2$)$_5$CO$_2$Me, DMF; (j) LiOH, H$_2$O; (k) cystamine•2HCl, BOP, THF; (l) 2N, HCl
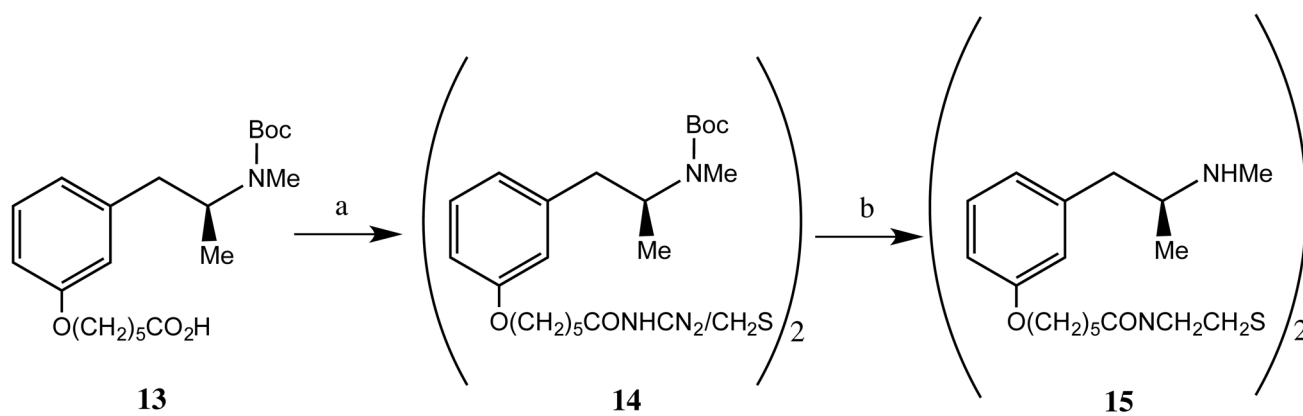
Scheme 2[a]

[a]Reagents (a) cystamine•2HCl, HOAt, EDC•HCl, Et$_3$N, DMF; (b) HCl, Et$_2$O
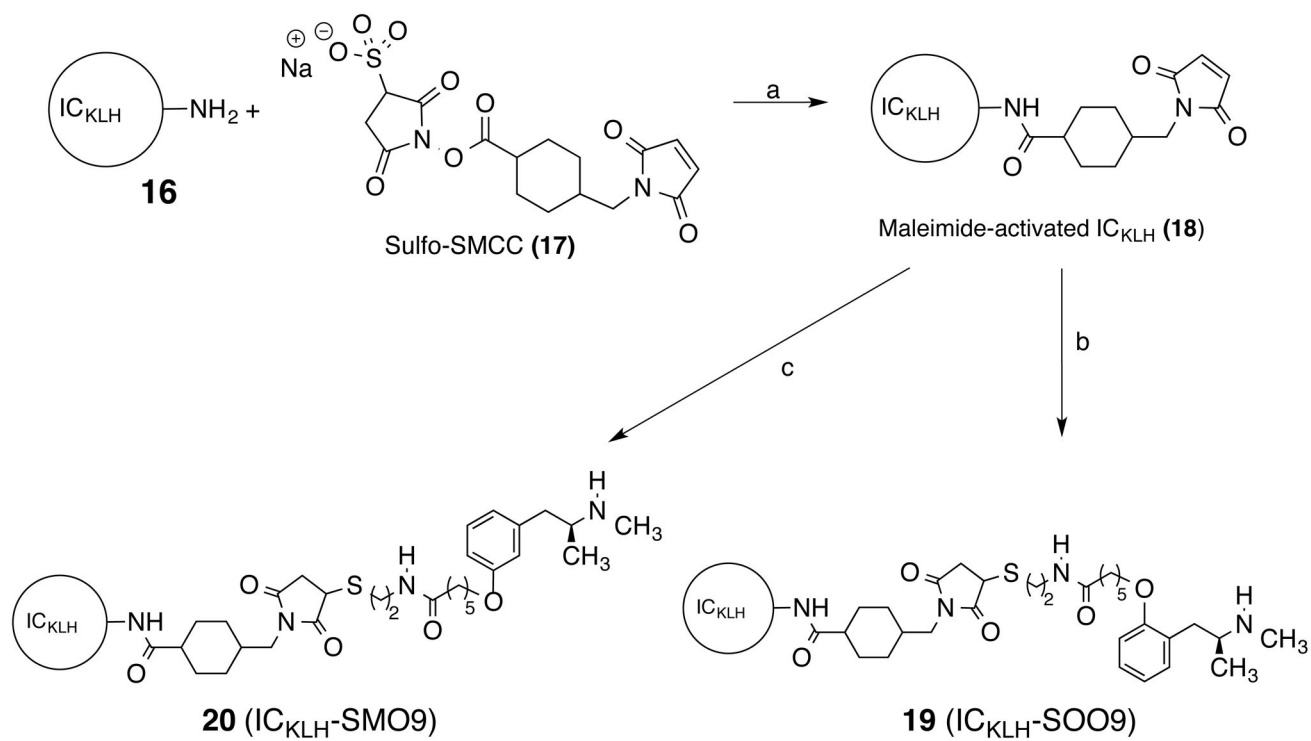
Scheme 3[a]

[a]Reagents: (a) H₂O; (b)TCEP, SSOO9 (**12**); (c) TCEP, SSMO9 (**15**)